João Monteiro Ferreira de Mira Coroa

Bachelor in Micro and Nanotechnologies Engeneering

Transfer of a Single Layer Graphene

Dissertation submitted in partial fulfillment
of the requirements for the degree of

Master of Science in
Micro and Nanotechnologies Engineering

Adviser: Prof. Dr. Stefan De Gendt, Full Professor, University of Leuven

Co-advisers: Dr. Steven Brems, Senior Researcher, imec

Prof. Dr. Rodrigo Paiva Fernão Martins, Full Professor, Faculty of Sciences and Technology, Nova University of Lisbon

FACULDADE DE CIÊNCIAS E TECNOLOGIA
UNIVERSIDADE NOVA DE LISBOA

September, 2017

Transfer of a Single Layer Graphene

This document was created using the (pdf)LaTeX processor, based in the "novathesis" template[1], developed at the Dep. Informática of FCT-NOVA [2].
[1] https://github.com/joaomlourenco/novathesis [2] http://www.di.fct.unl.pt

Genious is one 1% talent and 99% hard work...
Albert Einstein

Acknowledgements

In this section I would like to express my deepest gratitude to everyone involved in these last amazing 5 years that culminates with a master's degree in Micro and Nanotechnologies Engineering.

Firstly, I would like to thank my promotor, Prof. Dr. Stefan de Gendt, for the unforgettable opportunity he gave me by accepting me as his student and for all the advices that helped enrich this thesis. To my advisor Dr. Steven Brems, for taking responsibility of my person throughout my staying at imec, for all the first introductions at brand new topics and for all the meetings, opinions and laughs about our amazing friend graphene.

A big thanks to also my advisor, Prof. Dr. Rodrigo Martins, not only for the support during my staying in a foreign country but also for the important opinions about my work. Moreover, I would like to thank him and Prof. Elvira Fortunato for creating this amazing course of Engineering in Micro and Nanotechnologies.

Next, a very special thanks to Ken Verguts. Although your name is not in the first page you were a pillar in this thesis alongside with my promotor and advisers. Thank you, Ken, for all the successful and failed experiments, for all the runs you told me about, for the most excruciating pain I ever felt (Dodentoch, next year!), for all the laughs, late lunches, late afternoons working in the clean room but above all, thank you for all the things you taught me about graphene, our lovely and compliant friend. Also, I'm grateful to Kenny that in my first month helped more than ever adapting to Belgium, imec and even my home residence where I would be the next 7 months.

I would like also to acknowledge imec for receiving me as a student intern and for the excellent, top of-the-art conditions that allowed me to do an amazing research. A big thanks to all the NAME team that contributed with knowledge, challenges and ideas to the improvement of this thesis.

To all my friends and colleagues that helped me through this academic journey, and helped me study but also have fun. Because it all started with "dois amigos e um indiano" to my two friends, Tiago Gameiro and Shiv Bhudia, for the endless stories we shared together, the countless hangouts to study and to try to explain things to Shiv (but in the end he was getting higher grades), for all the parties, mts travels, it would not be the same without you. Also to my brother, Alexandre Fonseca, that showed me new expressions that only he knew like "é o pagode", for all the times he gave me shelter until the next day so I couldn't miss the test in early morning, for all the bad moments that he always knew how to turn in good moments. To Viorel Dubceac, my margem sul brother, for actually

making me "respect" margem sul and for all the talks with always inspiring words. To Sara Silvestre, my surfing partner that always had time for a quick surf no matter how busy her life was and by being a friend that I can always rely on. To Inês Martins, the little girl from Melisses with a big hearth that always has patience for us. To Jolu, David, Crespo, Chico, Xana, Vasco, Cátia, Sabrina, Caupi, Oliveira, Afilhada, Marco and all my nano friends that I "forgot" to mention here... all of you helped in your own special way. Thank you all.

Also, I would like to thank my tropas from Massamá for your unconditional support, love and coffes during the weekend. No matter how apart life take us you always can count on me and will be forever in my hearth.

To my Belgium family, Karen, Kostas, Panos, Pavlos, Yannis, Boren, Yahan, Eric and Ammar and my Erasmus boys, Ricardo, Marc and George. Thank you for providing great barbeques, bowling games, amazing trips and inspirational discussions. Belgium without you will never be the same.

Last, but not least, to my loving family, without them I could not be here. Thanks for all the help and the opportunity to have an education for the future. To my father, my mother, my brother, my uncles, Bé e Tia, my cousins, Marta e Madalena (as feias) and to my grandmothers, Avó Ilda e Avó Bia. You have always been in my thoughts, giving me energy and support for one more "cold" day in Belgium. This work is also yours, thank you.

Abstract

Graphene is a truly outstanding 2D material that holds the promise of revolutionizing the world with its many applications. All this expectation requires a high-quality graphene synthetized and transferred at large scale. Unfortunately, such industrial graphene is not currently feasible due the difficulty of the transfer even though its synthesis via chemical vapour deposition is becoming viable. Graphene is synthetized on a metal substrate, rendering graphene transfer an absolute necessity for use in electronic applications. A very recent transfer method, named direct transfer, has been proposed based on the electrochemical delamination that gives some hope in the matter. However, it is a method that still needs optimization by understanding its basis and by studying new target materials.

In this sudy, the intercalation of different ions/molecules during the electrochemical delamination is discussed. According to literature, during the electrochemical delamination H_2 bubbles produced at the cathode are responsible for delaminating the graphene. This work contradicts it, by saying that it is not the H_2 bubbles but rather charged species of the electrolyte. A cathodic and anodic study was made, where solutions with ions that would undergo electrochemical reactions in and outside the electrochemical window (EW) of water were tested. This thesis concluded that only if the cation/anion reaction is outside the EW or that the charged species will not react that the graphene would delaminate. Sodium hydroxide is the standard electrolyte used although it originates sodium contamination in graphene but now, electrolytes such as tetramethylammonium hydroxide and chloride and tetraethylammonium hydroxide can be used instead, avoiding at last sodium contamination in graphene devices.

Furthermore, this work also briefly discusses graphene adhesion to the target substrate and suggests, perhaps, hydrogen silesquioxane as target substrate due its capability of being transformed partially in SiO_2 after curing and avoiding the doping caused by the previous target substrate used.

Keywords: Graphene, direct transfer, electrochemical delamination, ion intercalation, chemical vapour deposition

Resumo

O grafeno é um material 2D extraordinário que promete revolucionar o mundo através das suas diversas aplicações. Todo este idealismo requer um grafeno de alta qualidade sintetizado e transferido em largas escalas. Infelizmente, tal grafeno industrial não é atualmente fiável devido à dificuldade existente em transferi-lo, apesar da sua síntese por deposição química de vapores estar-se a tornar plausível. O grafeno é crescido num substrato metálico, dando uma extrema importância à transferência do grafeno para aplicações electrónicas. Muito recentemente um método de transferência, denominado por transferência direta, foi proposto baseado na delaminação eletroquímica que pretende dar alguma esperança. Contudo, é um método que precisa de ser otimizado ao entender o seu funcionamento e ao estudar novos materiais para substrato alvo.

Neste estudo, a intercalação de diferentes iões/moléculas durante a delaminação eletroquímica é discutida. De acordo com a literatura, durante a delaminação electroquímica bolhas de hidrogénio são produzidas no cátodo e são responsáveis por delaminar o grafeno. Este trabalho contradiz isso na medida que não são as bolhas de hidrogénio, mas sim os iões do eletrólito. Um estudo catódico e anódico foi feito, onde soluções com iões que iriam ter uma reação eletroquímica dentro e fora da janela eletroquímica (JE) da água foram testados. Esta tese conclui que apenas quando a reação do catião/anião é fora da JE ou quando os iões não reagem é que o grafeno irá delaminar. Hidróxido de sódio é o eletrólito normalmente usado apesar da contaminação de sódio que causa ao grafeno mas, agora, eletrólitos como o hydróxido e cloreto de tetrametilamónio e hidróxido de tetraetilamónio surgem como alternativas, evitando por fim a contaminação por sódio em dispositivos de grafeno.

Para além disso, este trabalho também discute brevemente a adesão do grafeno ao substrato alvo e sugere possivelmente o hidrogénio silsesquioxano como substrato alvo devido à sua capacidade de se transformar parcialmente em SiO_2 após recozimento e ao facto de evitar a dopagem causada pelos substratos alvos já usados.

Palavras-chave: Grafeno, transferência directa, delaminação electroquímica, intercalação de iões, deposição química de vapores

Contents

List of Figures

List of Tables

Acronyms

0D	zero-dimensional.
1D	one-dimensional.
2D	two-dimensional.
3D	three-dimensional.
BLG	bi-layer graphene.
BZ	Brillouin zone.
CB	conduction band.
CMOS	complementary metal-oxide semiconductor.
CVD	chemical vapour deposition.
DCM	dichloromethane.
EW	electrochemical window.
FDTS	perfluorodecyltrichlorosilane.
FLG	few-layer graphene.
FWHM	full width at half maximum.
HSQ	hydrogen silsesquioxane.
IFW	interfacial water.
MLG	multi-layer graphene.
PC	polycarbonate.
PDMS	polydimethylsiloxane.
PMMA	poly-methyl methacrylate.

rpm rotations per minute.

SHE standard hydrogen electrode.
SLG single-layer graphene.

TCO transparent conductive oxide.

VB valence band.

Motivation

Since early ages I always felt a duty in preserving the world as we know it and, at the same time, in working towards a better and sustainable world for everyone. As I grew up I watched, enthusiast and perplex, the constant evolution and innovation of technology and the impact that did on our daily life. Rapidly I noticed that knowledge allied with technology it is what drives us to a brighter and exciting future.

The exploitation of our world's natural resources has always been a fundamental lever for technology success. A great example is the use of silicon in the semiconductor industry, a fundamental element for all of our integrated circuits (computers, cell phones and modern technology depends on it). However, with silicon pushed beyond limits in terms of miniaturization, we are coming to a technology barrier that challenges Moore's law. Thus, it is fundamental that we find alternatives and new ways to approach this obstacle. Scientists are constantly searching for a way to overcome, either by re-thinking the production process of devices, either by searching new materials that could replace silicon. Graphene reflect this potentiality in the means that represents a new path that could lead us to the next technology revolution, being one of the examples more discussed the supercapacitors that make our batteries obsolete. And this is only the tip of the iceberg, because graphene has extraordinary properties that, if applied with success, will revolutionize our world. However, high-quality graphene (required for these novel devices) is a material hard to synthetize and even more difficult to transfer, especially in larger scales so we can produce it industrially. With this mindset, my motivation becomes clear: transform this hope into reality.

Objectives

Single layer graphene has been called as the "wonder material" since its isolation in 2005 and its amazing properties promise to change the world as we know it. To integrate graphene in a novel architecture concept for CMOS technology it is necessary to transfer the graphene from its catalytic growth substrate to a dielectric substrate. The aim of this work is to study the intercalation of different ions/molecules during the electrochemical transfer process, which can be accelerated by attracting them via a potential. At the same time, it also intends to optimize the graphene direct transfer method by avoiding sodium contamination. Finally, it briefly discusses a different material, hydrogen silesquioxane, as a new target substrate for graphene direct transfer.

The transfer is said to be successful and with good quality if the following conditions are met:

- No additional damage on the graphene (wrinkles and cracks) during and after the transfer;
- No presence or minimal contamination of supporting material, solvents and other chemicals in the surface of the graphene or in the interface graphene-substrate;
- Scalability of the process to enable transfer of wafer scale graphene sheets (large production).

Chapter 1

Introduction

In this chapter the concept of graphene and how it emerged in our scientific world is explained. Additionally, it explores the unique structure of graphene and its amazing properties and thereafter the outstanding applications that have captured the attention and imagination of everyone.

1.1 Graphene

By entering the micro and nanoworld, size and dimension are the most crucial parameters when studying material properties. Two-dimensional (2D) materials are known for having only one (out of three) dimension restricted in size, usually in the vertical direction. A single atomic plane is considered a 2D crystal, whereas 100 layers of that should be considered as a thin film of a three-dimensional (3D) material. Therefore, they will differ in some properties from their bulk form, such as: optical and electronic properties (due the confinement of electrons) and chemical and mechanical response (due the geometry effect and high surface area) [1, 2].

Graphene appears as the most promising 2D structure for carbon materials due its potential technology impact. In simple terms, graphene is made of one atom thick layer of pure carbons atoms that are highly packed in a hexagonal honeycomb arrangement, and can be thought of as fused benzene rings without their hydrogen atoms [3], as illustrated in Figure 1.1.

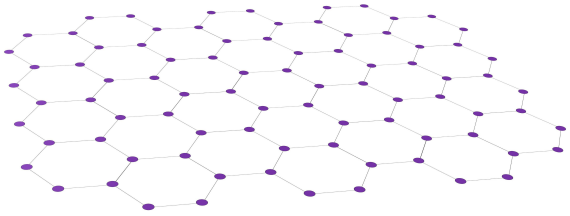

Figure 1.1: Graphene monolayer, a plane of carbon atoms.

Its first theoretical approach was done in 1974 by Wallace [4] and it was considered by the scientific community that strictly 2D crystals were thermodynamically unstable and could not exist [5, 6]. However, it was not until 2004 that A. Geim and K. Novoselov [7] proved the contrary and isolated for the first time a few layers of graphene at room temperature. One year later [8] they successfully narrowed it down to a single-layer graphene (SLG) by micromechanical exfoliation using the scotch tape method, a simple process but yet time consuming. Subsequently, their work led to more experimental activity regarding two dimensional materials [9, 10] and thanks to their groundbreaking experiments on graphene in 2004, they were awarded the 2010 Nobel Prize in Physics [11]. Bi-layer graphene (BLG) is considered to have two sheets of graphene and few-layer

graphene (FLG) has three to ten sheets whereas more than that is considered multi-layer graphene (MLG) and has the same electronic properties of graphite [12].

1.1.1 A Carbon structure

Carbon plays an intrinsic role in our nature, providing the basis for life on Earth. It is one of the few elements known since antiquity and the sixth element off our periodic table. Has a total of six electrons that occupy the atomic orbitals as $1s^2$, $2s^2$, $2p_x{}^1$ and $2p_y{}^1$. Being a tetravalent element (i.e. only the four exterior electrons participate in the formation of covalent chemical bonds) carbon atoms can likely bond together in different molecular/crystalline arrangements, forming the distinct carbon allotropes with dissimilar properties. The most common crystalline forms of carbon are graphite (the 'lead' of a common pencil) and diamond [13, 14].

As depicted in Figure 1.2 graphene is the basic building block of all graphitic forms. From there it can "wrap" itself into a zero-dimensional (0D) spherical C_{60} buckyball, "roll" itself into a one-dimensional (1D) CNT or it can be stacked into a 3D block of graphite, with an interplanar space of 0.335 nm [15].

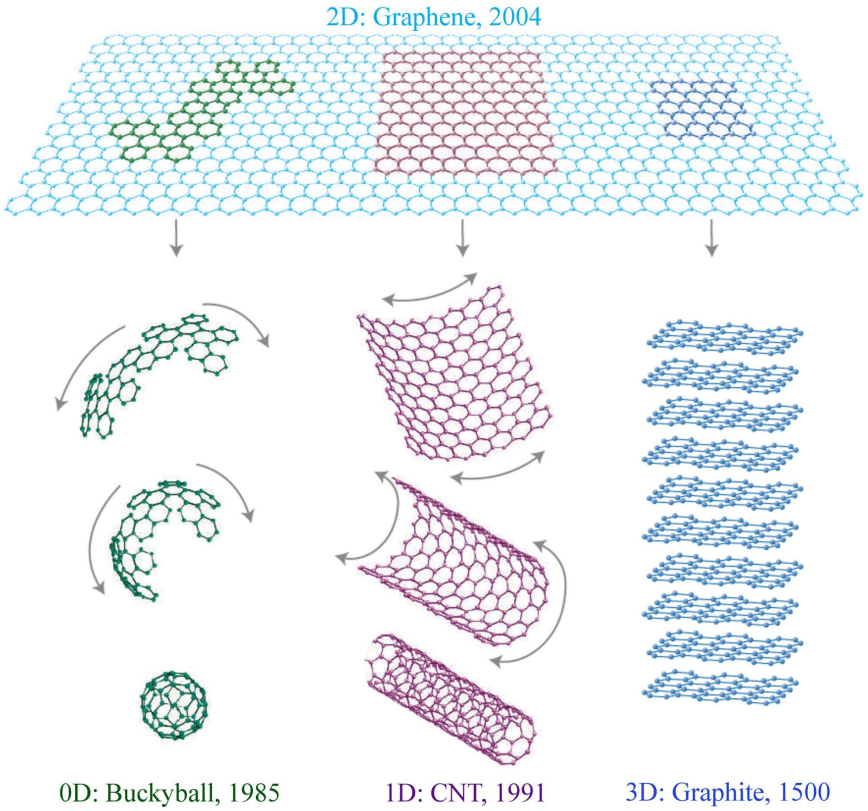

Figure 1.2: Mother of all graphitic forms. Graphene is a 2D building material for carbon materials of all other dimensionalities. It can be wrapped up into 0D buckyballs, rolled into 1D nanotubes or stacked into 3D graphite. Adapted from [16].

It is important to note that all these carbon allotropes result from a phenomenon

called hybridization, i.e. the concept of mixing atomic orbitals into new hybrid orbitals suitable for the pairing of electrons to chemically bond to other atoms. There are three types of hybrid configurations: sp^3, sp^2 and sp. In the case of carbon, its allotropes distribute themselves in a tetragonal sp^3 configuration (diamond), in a trigonal sp^2 configuration (carbon nanotubes, buckyballs and graphite) and in a planar sp configuration (acetylene). In particular, graphene is a single-layer sheet of sp^2 carbon atoms with a carbon-carbon bond length of 0.142 nm [17, 18]. A sp^2 hybridization occurs when one s-orbital is combined with only two 2p-orbitals, specifically p_x and p_y (see Figure 1.3a). By this, the sp^2 orbitals contribute together to a planar assembly with an angle of 120° between them where the additional p_z orbital is perpendicular to them [19], as shown in Figure 1.3b.

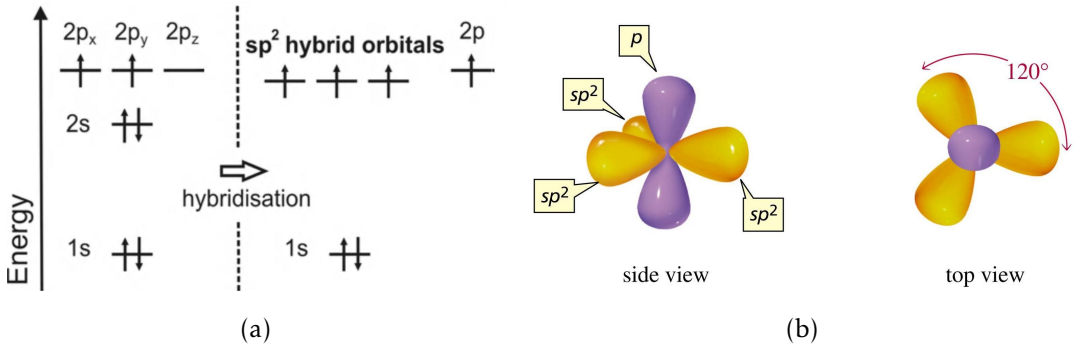

Figure 1.3: (a) Atomic orbital diagram of a carbon atom hybridizing to a sp^2 configuration (adapted from [20]) and (b) its resultant trigonal planar geometry (from [21]).

1.1.2 Electronic and Crystal structure

Regarding the electronic structure of graphene, the sp^2-orbitals are responsible for forming a strong covalent bond (σ-bond) between the three neighboring atoms inducing the planar hexagonal honeycomb structure of graphene. The C-C bonding is enhanced by a fourth bond (π-bond) associated with the overlap of p_z orbitals. The electronic properties are determined by the bonding π and π^* orbitals, forming the electronic valence and conduction bands. The dispersion of the pi electrons in graphene was first calculated within the tight-binding approximation in 1947 [4] (see Figure 1.4a) and they are responsible for most of the electronic and chemical properties of graphene [15].

Concerning the crystal structure, the unit cell of graphene has a basis of two non-equivalent carbon atoms (A and B) and graphene has a honeycomb bipartite lattice structure with two corresponding triangular sublattice sites (see Figure 1.5a). The lattice vectors (known as the real space vectors, a_1 and a_2) and the reciprocal-lattice vectors (denoted as the Fourier transformation of the real space vectors, b_1 and b_2) can be written in cartesian coordinates as the following, where $a = 0.142$ nm [3, 14, 23]:

$$a_1 = \frac{a}{2}(3,\sqrt{3}) \quad ; \quad a_2 = \frac{a}{2}(3,-\sqrt{3}) \quad ; \quad b_1 = \frac{2\pi}{3a}(1,\sqrt{3}) \quad ; \quad b_2 = \frac{2\pi}{3a}(1,-\sqrt{3})$$

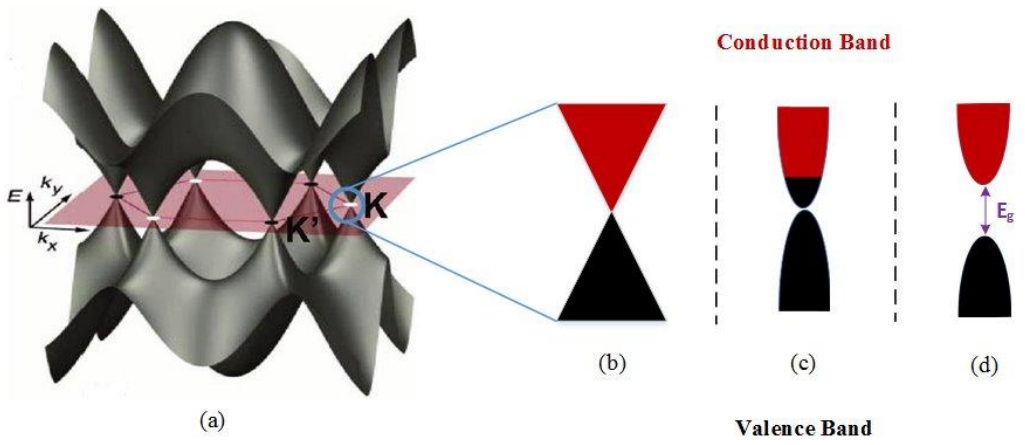

Figure 1.4: (a) Energy dispersion of single-layer graphene obtained via nearest neighbour approximation. Band structure of (b) graphene, (c) metals and (d) insulators (for E_g > ~4 eV) or semiconductors (for E_g < ~2 eV). Adapted from [22].

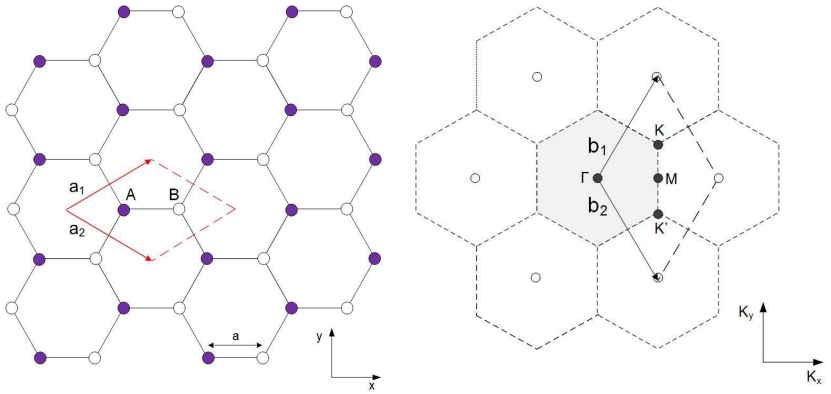

Figure 1.5: Crystal structure of graphene: (a) hexagonal lattice of graphene in real space with basis vectors a_1 and a_2. The unit cell is marked in red. It contains two nonequivalent carbon atoms A and B, each of which span a triangular sublattice; (b) Reciprocal lattice (dashed) with reciprocal lattice vectors b_1 and b_2. The first Brillouin zone is highlighted in grey and the high symmetry points Γ, M, K and K' are indicated. Adapted from [20].

The first Brillouin zone (BZ) can be defined as the primitive cell in the reciprocal space, represented in Figure 1.5b. Furthermore, the unit cell of graphene in the real space is transcribed to the first BZ with four independent high-symmetry points. Of particular importance for the physics of graphene are the two points K and K' at its corners. At these points, denominated Dirac points, something extraordinary occurs: the conduction band (CB) and the valence band (VB) touch each other in a conical energy spectrum with a linear dispersion, forming a structure known as Dirac cone (see Figure 1.4b). For this reason, graphene is often called a zero-gap semiconductor at these points and the charge carriers (electrons or holes) are considered massless Dirac Fermions (i.e., same velocity and absolutely no inertia), exhibiting exceptional high mobilities [24]. These Dirac cones

are rather unique strucutures since there is no partially-filled band, unlike the metals (see Figure 1.4c), but no gap, unlike the insulators and semiconductors (see Figure 1.4d) [3, 10].

1.1.3 Stacking

As pointed out in Section 1.1, graphene can be quantified accordingly to the amount of layers existing (SLG, BLG, FLG or MLG). When stacked, carbon atoms can be set in different ways [25–27]:

- Hexagonal or AA stacking, where the carbon atoms of both layers are situated on top of each other;
- Bernal or AB stacking, which have one layer shifted with respect to the other layer - one corner of the hexagons of the top sheet is located above the center of the hexagons of the bottom sheet. Is the lowest energy stacking and therefore the most common form in single crystal graphite and FLG;
- Turbostratic stacking, where one layer is rotated with respect to the other by an angle of $\theta \neq$ n 60° where n = 0, 1, 2...;
- Rhombohedral or ABC stacking (only for more than two layers), where the third layer has no overlap with the first nor with the second layer.

Depending on the number of layers and in the stacking sequence, graphene can have its electronic properties changed considerably, altering its band structure itself. For example, AB stacked bi-layer graphene is considered the only tunable gap (i.e., it can develop into an energy gap if it is subjected to an external perpendicular electric field [28]) semiconductor and shows a gapless state with parabolic bands (quadratic dispersion) instead of the linear dispersion in SLG. In contrast with SLG, charge carriers in BLG have finite mass and are called massive Dirac fermions [29–31]. Although the different electronic properties obtained by stacking graphene, only SLG is in the interest of this thesis.

1.1.4 Properties

After the first report of graphene's exceptional electronic properties in 2005 there has been a gold-rush in exploring more amazing properties that graphene might have to offer. So far, there are some remarkable properties reported (see Table 1.1) that provided the graphene the title of the thinnest, most flexible and strongest material known to humankind. Graphene also shows room-temperature ambipolar characteristics, where charge carriers can be alternated between holes and electrons depending on the nature of the gate voltage [32, 33].

Table 1.1: Some properties of graphene.

Properties	Values	Reference
Carrier Mobility	350,000 $cm^2v^{-1}s^{-1}$	[34]
Optical Transparency	97.7 %	[22]
Thermal Conductivity	5,000 $Wm^{-1}K^{-1}$	[35]
Tensile Strength	130 GPa	[36, 37]
Elastic Modulus	1.1 TPa	[36, 37]

1.1.5 Applications

A close look to the values represented in Table 1.1 shows the huge potential of graphene. Not only it has the best thermal conductivity of any known material but also exhibits the highest carrier mobility at room temperature, with values ~100 times greater than silicon and even ~10 times better than the state-of-the-art high mobility group III-IV semiconductors [38, 39], holding the expectation of even reaching extremely large values of 3×10^6 $\mathrm{cm^2\,V^{-1}\,s^{-1}}$ [40]. However, due to the zero bandgap, it is not possible to switch off devices with channels made of purely graphene, limiting the on-off current. There are some approaches in trying to open a bandgap [41–43]) although it is a complex method. Nevertheless, this does not rule out radio-frequency or analogue applications, such as amplifiers and transmitters, being a promising candidate for higher maximum operating frequencies (>100 GHz) [44].

Graphene's conductivity can also be changed easily either by chemical doping or by an electric field, making it ideal for sensor applications. A scalable gas sensor from chemically derived graphene has already been demonstrated [45]. Furthermore, graphene also appears as a new generation of transparent conductors when trying to account the emerging necessity to replace existing transparent conductive oxide (TCO) materials and the growing market towards bendable electronics. Here, flexible graphene based electrodes provide critical performance advantages due the combination of a high charge carrier mobility, high transparency in the visible region and the additional flexibility and high stretchability while the standard TCOs are brittle due their ceramic nature, hard to obtain and expensive to manufacture reflecting in their high prize. However, efforts to make transparent conducting films from graphene have been hindered by the lack of efficient methods for the synthesis, transfer and scalability of graphene at a quality required for applications [46–48].

Regarding energy applications, there is a global demand for more and more energy with minimal damage to the environment. Graphene with its high electrical conductivity, large surface area, interlayer structure and being environmental friendly makes it a potential contender as a material in electrochemical energy systems, such as supercapacitors [49, 50], lithium ion batteries [49, 51], fuel cells [49, 52] and solar cells [49, 53]. Moreover, its outstanding mechanical properties, large specific surface area and two dimensional high aspect ratio geometry make it ideal as a nanofiller in composite materials [54].

Chapter 2

Experimental Methods

This chapter briefly reviews the various methodologies for fabricating graphene before finally depicting the transfer process of graphene and later-on its characterization.

2.1 Synthesis

Since the first isolation of graphene by scotch tape in 2005 several other techniques have been established for graphene synthesis. These new processing routes came along with efforts for efficient synthesis of large-scale graphene and can be seen as two main approaches: top-down (a bulk material is 'carved' out to create nano-sized graphene structures) and bottom-up (graphene is built from scratch, i.e., self-assembly of carbon atoms). An overview of graphene synthesis techniques is shown in the flow chart in Figure 2.1. Each one has its advantages and drawbacks depending upon the final application of graphene. Chemical vapour deposition (CVD) is the one that stands out due its high--quality, large-area scalable graphene and because it is a compatible method for future complementary metal-oxide semiconductor (CMOS) technology [55]. Nevertheless, its bottleneck is that graphene synthesized by CVD should be transferred from the catalyst metal substrate (such as Ru, Pt, Ni and Cu [56]) to a dielectric substrate for application to a variety of fields, making the transfer a very important and determinant step for having high-quality graphene [18].

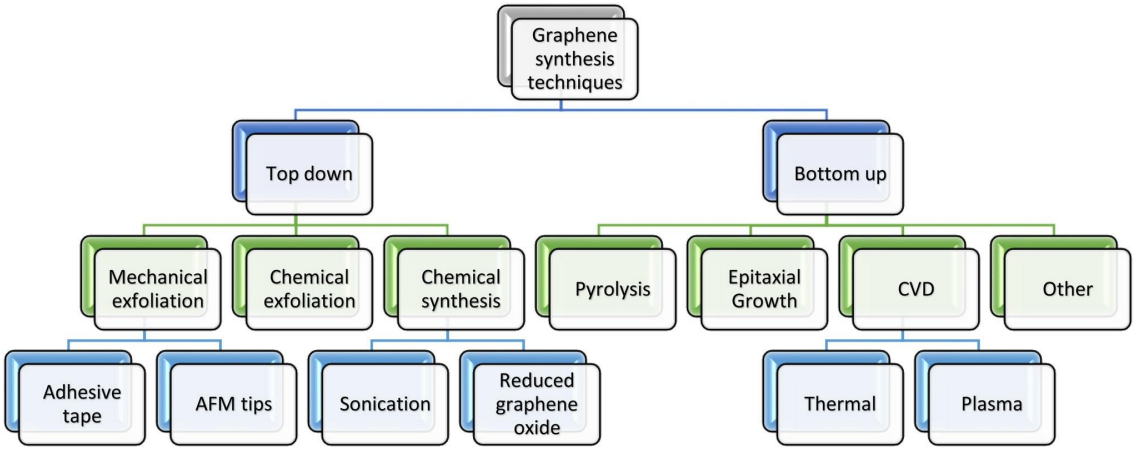

Figure 2.1: A process flow chart of graphene synthesis. From [18].

The recipes for growing graphene are optimized with the objective of growing only SLG. Graphene is grown both on Al_2O_3(0001)/Pt(111) wafers and Pt foils (Alfa Aesar, 50 μm thick, 99.99 % trace metals basis) depending on the type of transfer that will be used and also at different conditions since they are different in terms of thickness and crystallinity. The growth was done in a vertical cold-wall Aixtron Black Magic 6" CVD system, with the reactor pressure at a constant 750 mbar throughout the full process.

In the case of the Pt on sapphire wafers, the reactor was heated in 850 sccm hydrogen atmosphere untill 1080 °C. Next, 6 sccm methane was introduced into the chamber for 30 min. Finally, the reactor was cooled down to room temperature at a cooling rate of 15 °C min^{-1} under a methane and hydrogen ambient with a methane to hydrogen ratio of 3:850 sccm. For the Pt foils the reactor was heated in 800 sccm hydrogen atmosphere until 980 °C. Then 5 sccm methane was introduced to the chamber for 20 minutes. To end, the reactor was cooled down to room temperature at a cooling rate of 15 °C min^{-1} in a methane to hydrogen ratio of 4:800 sccm.

2.2 Transfer

As pointed out in the previous section, CVD graphene needs to be transferred to a target substrate for most applications and basic research. A variety of transfer routes have been reported [57] and the typical adopted approach to separate graphene from its growth metal substrate is through chemical etchants to completely dissolve the metal, resulting in some unfortunate drawbacks due the etchant used, such as: environmental and costs issues, damage (defects, excess doping, etc.) and metal contamination in the graphene and loss of the growth substrate. Usually, graphene is supported by a polymeric film while the metal is being removed and the resultant polymer/graphene complex (named from this point forward as 'stack') is then placed on the target after which the polymer is removed by a solvent [58–60].

It was not until a few years back [61, 62] that a transfer technique based on an electrochemical delamination was proposed where the catalyst foils are not consumed and can be recycled for re-growing graphene. In this approach electrolysis takes place, by which charged ions (cations or anions) are formed when an electric current (generated by the cathode and anode) is passed through an ionic substance (electrolyte). The half reactions on the cathode (negative side) and on the anode (positive side) depends on the electrolyte used, more specifically in its pH (see equations 2.1 to 2.6).

According to the literature [61–63], electrochemical delamination is a mechanism that counts with the mechanical separation of graphene from the metal substrate only by H_2 bubble formation at the cathode of an electrolytic cell. Previous studies [64], also indicate that a step of water intercalation is crucial in order for this method to work. A thin layer of water between the graphene and the metal substrate (interfacial water (IFW))

helps the hydrogen bubbles intercalate and drive the delamination forward. However, delamination by hydrogen bubbling depends on several parameters such as sample size, the cell overpotential, type of electrolyte and its concentration, etc., and although it is a simple mechanism is a process that is not quite yet understood [58]. After the delamination, the graphene is transferred to the target substrate via two standard methods [56]: a dry-transfer where there is no water between the final target substrate and the graphene, and a wet-transfer where there is. The disadvantage of these methods remains in the need of a polymeric film on top of the graphene, so it can endure the process of the transfers, causing future polymer contamination when tried to remove it. Very recently [64], a new approach based on the electrochemical delamination of graphene without the need of a polymeric film was proposed, entitled direct transfer. All of them have their own route that will be explained in the following sub-sections.

Alkaline solutions

$$\text{Cathode: } 2\,H_2O\,(l) + 2\,e^- \longrightarrow H_2\,(g) + 2\,OH^-\,(aq) \tag{2.1}$$

$$\text{Anode: } 4\,OH^-\,(aq) \longrightarrow O_2\,(g) + 2\,H_2O\,(l) + 4\,e^- \tag{2.2}$$

$$\text{Overall reaction: } 2\,OH^-\,(aq) \longrightarrow 2\,H_2\,(g) + O_2\,(g) \tag{2.3}$$

Acidic solutions

$$\text{Cathode: } 2\,H^+\,(aq) + 2\,e^- \longrightarrow H_2\,(g) \tag{2.4}$$

$$\text{Anode: } 2\,H_2O\,(l) \longrightarrow O_2\,(g) + 4\,H^+\,(aq) + 4\,e^- \tag{2.5}$$

$$\text{Overall reaction: } 2\,H_2O\,(l) \longrightarrow 2\,H_2\,(g) + O_2\,(g) \tag{2.6}$$

2.2.1 Direct Transfer

Figure 2.2 shows the basic procedure for direct transfer. Graphene is grown in a Al_2O_3 (0001)/ Pt(111) wafer that limits the multilayer growth and smooths the surface, to prevent the trapping of water/air molecules at the target/graphene interface. Likewise, the target substrate has to be hydrophobic so it can repeal any water while doing the transfer and avoid trapping. Then a dry-bonding is made between the sample and the hydrophobic target substrate at a pressure of 250 kPa. The electrolyte is introduced in the structure until it is completely filled and the electrolysis takes place to delaminate the graphene. At the same time, the pressure is gradually decreased where the transfer happens due the combination of the promoted water intercalation (IFW) between graphene and the Pt sapphire wafer and the prevented water intercalation (due the hydrophobic target substrate) between the graphene and the target substrate [64].

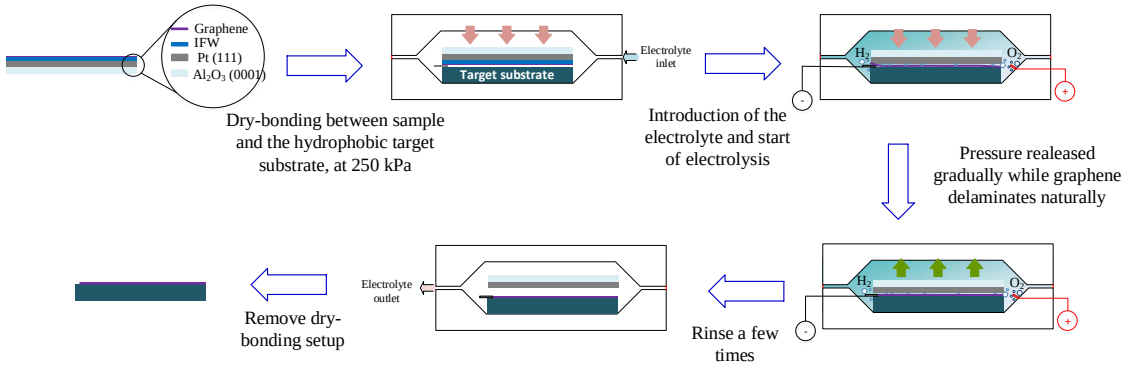

Figure 2.2: Process route for a direct transfer based on the electrochemical method with the sample as cathode and a bare Pt foil as anode.

2.2.2 Wet-Transfer

Figure 2.3 illustrates the steps for the wet-transfer. During electrolysis, the sample is carefully introduced in the electrolyte at the same time the stack is being delaminated. After a successful delamination, the stack is fished with a dummy substrate and transferred to water a few times in order to rinse it. Then, it is fished with the hydrophilic target substrate (for an easier fishing and to avoid future solvent intercalation) and left to dry at 50 °C. Finally, the polymer is removed by a solvent and the transfer is complete. It is a process that is entirely dependent on the natural delamination of graphene [56].

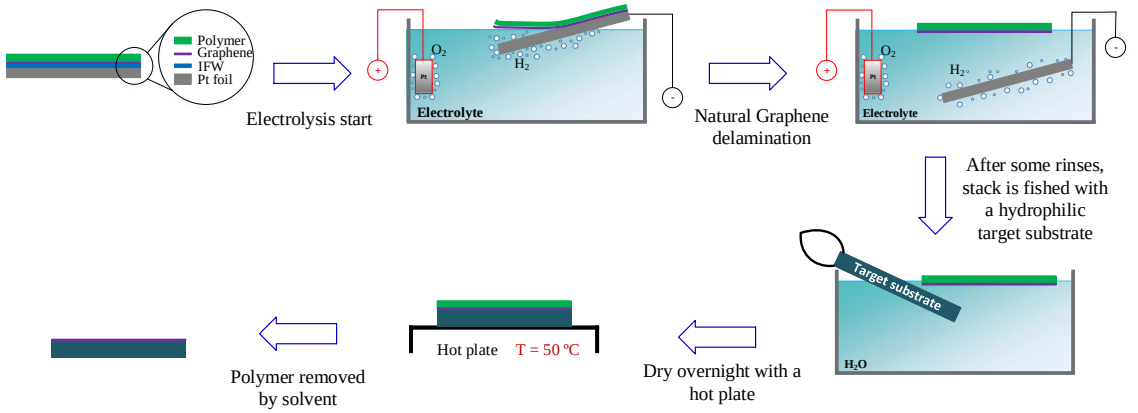

Figure 2.3: Process route for a wet-transfer based on the electrochemical method with the sample as cathode and a bare Pt foil as anode.

2.2.3 Dry-transfer

Figure 2.4 depicts the overall process for the dry-transfer. This time, the sample has a polydimethylsiloxane (PDMS) of 1 mm thickness on top of the polymer that allows a more carefree handling. The electrolysis starts with the appropriate voltage and after some time the graphene delaminates naturally and the PDMS is picked up with the tweezer. In case the complex stack/PDMS is not detached naturally, a minimal mechanical force

is added with the tweezer in order to promote the delamination. Then some rinses with water are made, it is usually left to dry at room temperature over-night and later-on is applied to the hydrophilic target substrate. By heating up the structure above the glass transition temperature of the support layer it is possible to peel of the PDMS leaving the stack behind attached to the target substrate. Finally, the polymer is removed by a solvent and the transfer is complete. The big advantage of this method over the wet-transfer rely in preventing ions at the graphene/target substrate interface since it does not get wet. However, this method often compromises the structural integrity of graphene making the wet-transfer a better method to obtain an uniform graphene layer capable of being used and characterized [56].

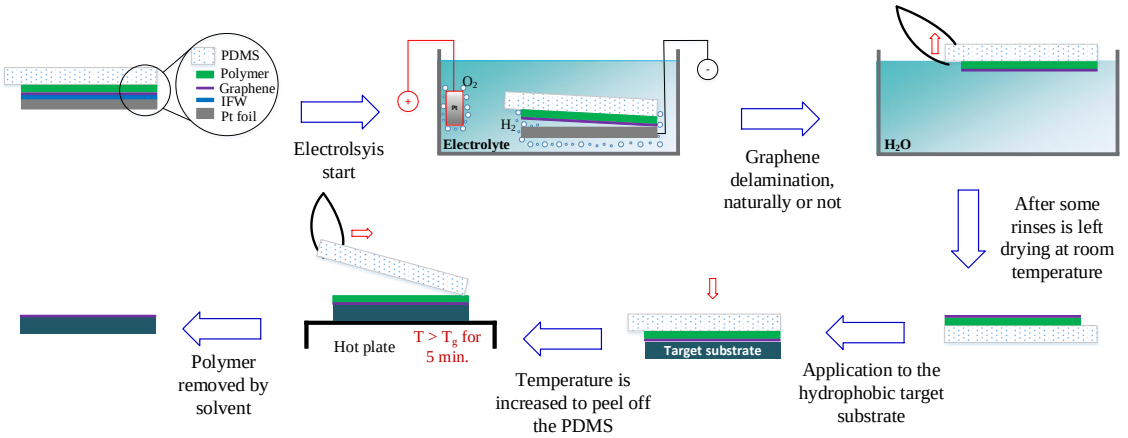

Figure 2.4: Process route for a dry-transfer based on the electrochemical method with the sample as cathode and a bare Pt foil as anode.

2.3 Characterization

The characterization of the resultant transfer is an important step to verify the quality and the condition of the SLG. Different characterizations like optical microscopy, Raman spectroscopy, X-ray photoelectron spectroscopy and atomic force microscopy make all together a powerful tool to achieve that. In this study it was used two main methods: optical microscopy and Raman spectroscopy.

2.3.1 Optical Microcope

Figure 2.5 shows an example of a wet transferred graphene with sodium hydroxide (NaOH) as an electrolyte. The microscopic images allow us the first look and estimation of the quality of the graphene. With it, it is possible to identify the presence of graphene (see Appendix A for more details), as well as cracks, polymer contaminations, wrinkles and even if it is scrolled or with more than one layer (BLG or FLG).

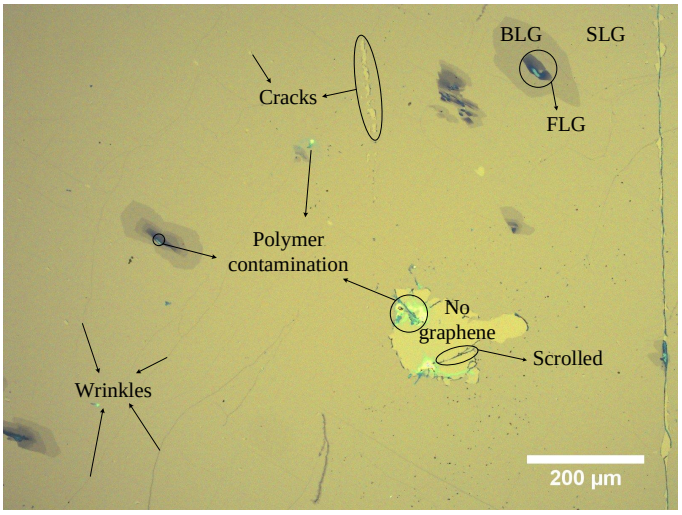

Figure 2.5: Optical microscopy image after a wet graphene transfer using NaOH as electrolyte.

2.3.2 Raman spectroscopy

Raman spectroscopy is a vibrational technique that is extremely sensitive to geometric structure and bonding within molecules. By identifying vibrational modes using only laser excitation, Raman spectroscopy has become a powerful, noninvasive method to characterize graphene and related materials. In graphene, the spectra exhibit a relatively simple structure characterized by two principle bands designated as the G and 2D bands. A third band, the D band, may also appear in graphene when defects within the carbon lattice are present [65, 66]. The band positions are illustrated in Figure 2.6.

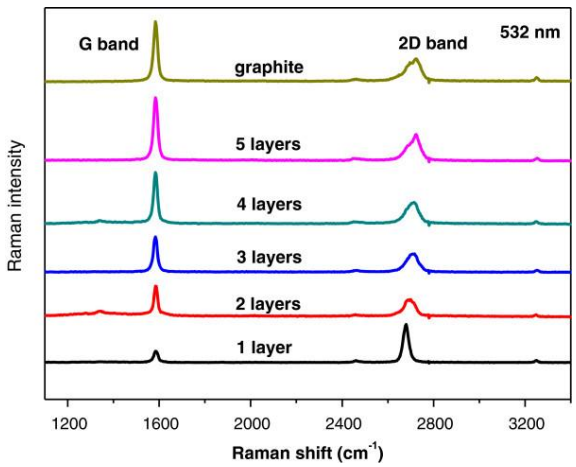

Figure 2.6: Comparison of Raman spectra at 532 nm for few-layer graphene. From [67].

Clearly, these Raman spectra demonstrate the ability to distinguish between the different graphene layer thickness at an atomic layer resolution , although its utility relies in differentiating SLG from BLG and FLG through the position of the G peak and the spectral features of the 2D band. Yet, this thesis only focus in SLG where each band can give us some details about it [65, 66]:

- The D band (~1350 cm^{-1}) is known as the disorder band or the defect band and is associated to a presence of a sp^3 carbon. If the D band is significant it means that there are a lot of defects in the material. The smaller the ratio between the intensity of the D peak with the G peak (I_D/I_G) the less defects are present. This thesis aims for a high-quality graphene which has this peak absent;
- The G band position (~1580 cm^{-1}) is an in-plane vibrational mode involving the sp^2 hybridized carbon atoms that comprises the graphene sheet;
- The 2D band (~2690 cm^{-1}) is the second order of the D band, and is the result of a two phonon lattice vibrational process. Unlike the D band, it does not represent defects but rather appear as a strong band in graphene. The full width at half maximum (FWHM) of this band can give an important clue about the flatness of the graphene: smaller the FWHM smoother is the surface and consequently the more mobility attained, above 40 cm^{-1} graphene start to have large strain variations [68].

In this work, graphene is characterized using a Horiba Labram HR with a green laser (λ = 532 nm), recording intensities from υ= 1250 cm^{-1} to υ= 2850 cm^{-1}.

Chapter 3

Results and Discussion

This chapter summarizes all the work done regarding the transfer of graphene. First the direct transfer is approached as an alternative and innovative technique along with its advantages and obstacles. Secondly, to try to overcome those obstacles, a detailed study of electrolytes is made with the dry- and wet-transfers. Finally, graphene's adhesion to the target substrate is discussed, namely with hydrogen silsesquioxane, since it is a critical factor in the transfer.

3.1 Starting Material

After the growth, the Pt sapphire wafers and Pt foils were also put in water at 50 °C for 24h in order to create the IFW layer. Only then, the samples were considered ready to transfer.

3.2 Direct Transfer - issues

The direct transfer shows up as an exciting new method for graphene transfer. It requires few handling, does not need support/polymeric material and has the possibility to be scalable. It combines the electrolysis from the electrochemical delamination with a home--made bonding setup. The structure needed is minutely depicted in Figure 3.1, with all the important components although it still needs optimization. Apart from depending completely in the natural delamination of graphene, two major aspects are important for the success of this transfer, being the growth substrate and the target substrate. As said in sub-section 2.2.1 the growth substrate has to be sapphire (Al_2O_3 (0001)) with platinum oriented in the (111) direction. This way the multilayers are considerably reduced because there are no grain boundaries in the platinum (contrary to the Pt foils) and the surface is almost completely flat helping with the adhesion between the graphene and the target substrate since it will trap less water/air molecules. At the same time, the target substrate has to be hydrophobic (see Appendix A) to repel the electrolyte and minimize its intercalation between graphene and the target substrate.

Sodium hydroxide is the standard electrolyte used by the literature [56, 59, 61, 69]. As soon as the 250 kPa are applied, NaOH is introduced until the chamber is filled. Then the electrolysis begin with a voltage set to -2.5 V and after 3 minutes, the pressure is decreased by 10 kPa per minute. Figure 3.2 shows the resulted graphene previously

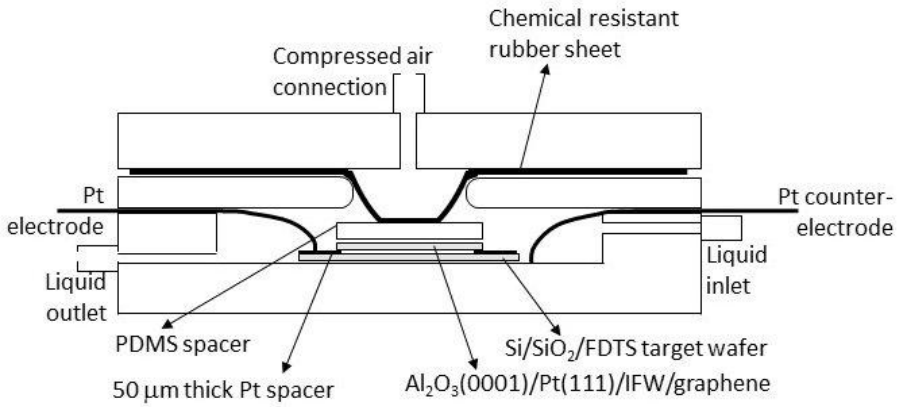

Figure 3.1: Scheme of a home-made bonding setup for a direct graphene transfer to a hydrophobic wafer. 50 µm thick Pt spacers at the edge of the wafers are used to electrically contact the Al_2O_3/Pt/graphene layer and to separate the growth wafer from the target wafer. Compressed air is used to bond graphene on top of the target wafer. A Pt working electrode connected to the Pt growth template and a Pt counter electrode is used to construct the electrochemical cell. A liquid inlet and outlet are included to introduce the electrolyte and allow the rinsing. From [64].

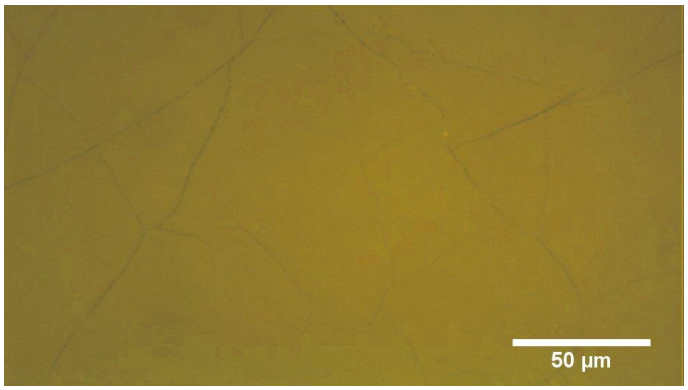

Figure 3.2: Optical microscopy image after a direct graphene transfer. From [64].

obtained in another study with a very clean and effective transfer (free of polymers and cracks). However, this transfer still has some issues such as sodium contamination and doping in the graphene, caused, respectively, by the electrolyte used [70, 71] and by the hydrophobic substrate [72], which ultimately decreases one of the prestigious properties of graphene: its mobility. Therefore an electrolyte study and a substrate study was made in order to try to give some answers to these problems.

3.3 Electrolyte Study

As discussed in Section 2.2, the electrochemical method is a technique that depends on the electrolytic cell. Actually, not every electrolyte, despite being conductive and therefore contributing with charged ions to the process, helps in graphene delamination [58]. In order to eliminate sodium contamination, it is important to understand why NaOH works and also to have an idea of which electrolyte would work for further process optimization.

The sapphire wafers with platinum are an expensive material to obtain and hence the standard electrochemical methods (dry-and wet-transfers using graphene grown on Pt foils) are used from this point onwards to do a close study concerning the electrolytes and their influence in the transfer process. In spite of the big advantage of the dry-transfer over the wet-transfer, it is a method that often fails in retaining the macroscopic structural integrity of graphene (i.e., broken and scrolled graphene is usually present) mainly due the bad adhesion between graphene and the target substrate, later discussed. Nevertheless, a dry-transfer was done first to give an idea about the natural delamination of graphene (by the aid of the mechanical force or not). Then, if it was indeed a natural process the wet-transfer was done resulting in a more uniform, undamaged transferred graphene. All the remaining conditions were maintained the same throughout the experiments so it could not affect the results, such as:

- The target substrate was always a silicon/silicon dioxide (Si/SiO_2) wafer, pretreated with NH_4OH: H_2O_2: H_2O (see Appendix A);
- The support layer used was always polycarbonate (PC) (see Appendix B);
- All the electrolytes had a concentration of 0.2 M in 1L of H_2O.

This discussion will be divided in two main approaches:

1. Sample as cathode: where the cations are attracted to the negatively charged electrode, like represented in Figures 2.3 and 2.4;
2. Sample as anode: where the anions are attracted to the positively charged electrode.

3.3.1 Sample as cathode

The following electrolytes were used: NaOH, sodium nitrate ($NaNO_3$), sodium sulfate (Na_2SO_4), potassium sulfate (K_2SO_4), sulfuric acid (H_2SO_4), cerium sulfate ($Ce(SO_4)_2$), nitric acid (HNO_3), ammonium hydroxide (NH_4OH), tetramethylammonium hydroxide and chloride (TMAH and TMACl) and tetraethylammonium hydroxide (TEAH). Figure 3.3 shows them with the respective cation that is being attracted to the interface. Note again that all these electrolytes are conductive and adequate for the process of electrolysis.

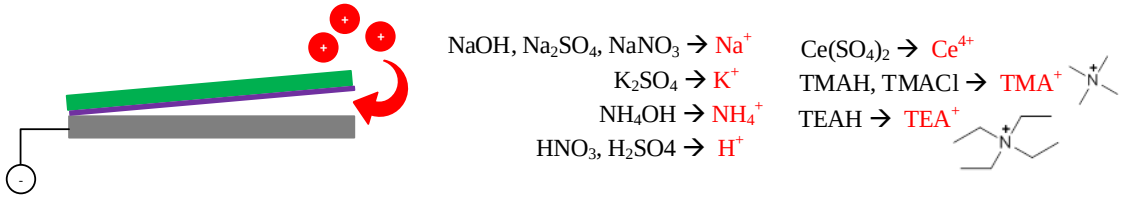

Figure 3.3: Cations of an electrolyte being attracted by the electrode (cathode). The cations of each electrolyte are marked in red.

With NaOH, TMAH and TEAH the delamination of graphene in the dry-transfer is completely smooth where it is just needed to pick-up the PDMS from the solution after 3 minutes of electrolysis at -2.5 V. Although it shows a very natural delamination, the transferred graphene appears broken and scrolled with the presence of a lot of cracks. This happens mainly due the bad adhesion between graphene and the substrate, since during the removal of the polymer the solvent intercalates under the graphene (between the treated target substrate and the sheet of graphene) and removes it [73–75]. This situation happens more frequently when it is done the dry-transfer because of the application and removal of the PDMS: air bubbles trapped in between the surfaces and/or too much stress applied when transferring the stack to the treated target substrate might crack the polymer/graphene and promote solvent intercalation. In contrast, the wet-transfer does not need assistance reflecting in much better results (no/few cracks and uniform graphene) since the delamination is very smooth, fast and with the same potential applied (see figs. 3.4a to 3.4c). The Raman spectra reveals a high-quality graphene (low I_D/I_G peak ratio) with FWHM values corresponding to a not so smooth high-quality graphene.

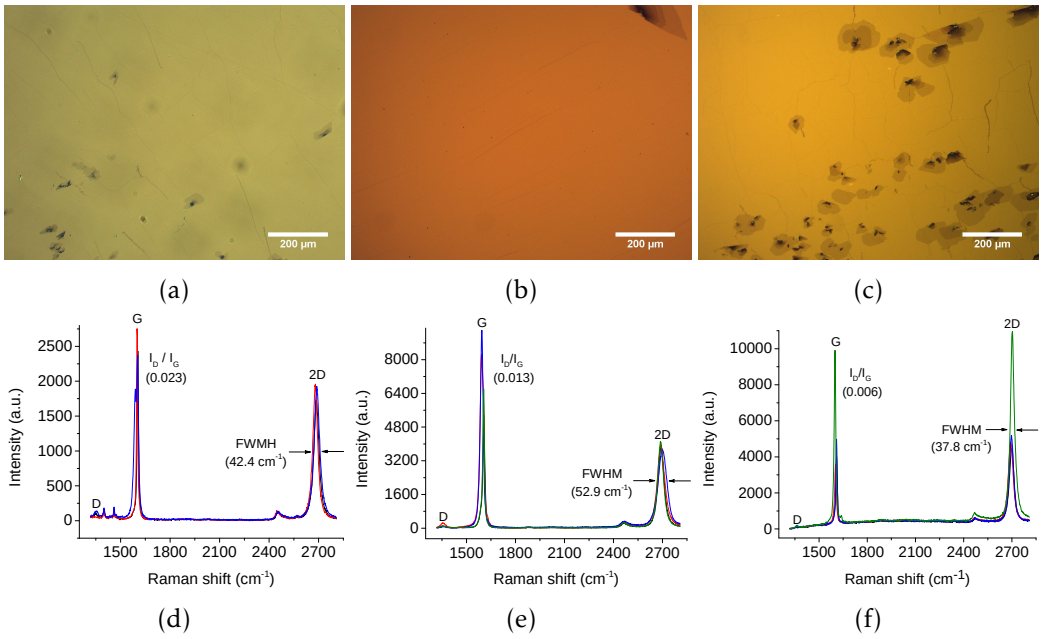

Figure 3.4: Optical microscopy images after a wet graphene transfer with (a) NaOH, (b) TMAH and (c) TEAH and their respective (d, e, f) Raman spectra measured in four different points.

The same results are produced with $NaNO_3$, Na_2SO_4, K_2SO_4, and TMACl (Figures 3.5a to 3.5c and 3.5g) for the dry- and wet-transfer even though the delamination is longer than with the first electrolytes discussed. Regarding the quality of graphene, all the Raman spectra present a low I_D/I_G peak ratio (< 5%) proving a high-quality graphene although with some strain variations related with high FWHM values.

When trying the electrochemical method with the remaining electrolytes, delamination gets more complicated. For H_2SO_4, HNO_3 and NH_4OH it was a difficult delamination in the dry-transfer where the PDMS had to be pulled with some mechanical strength

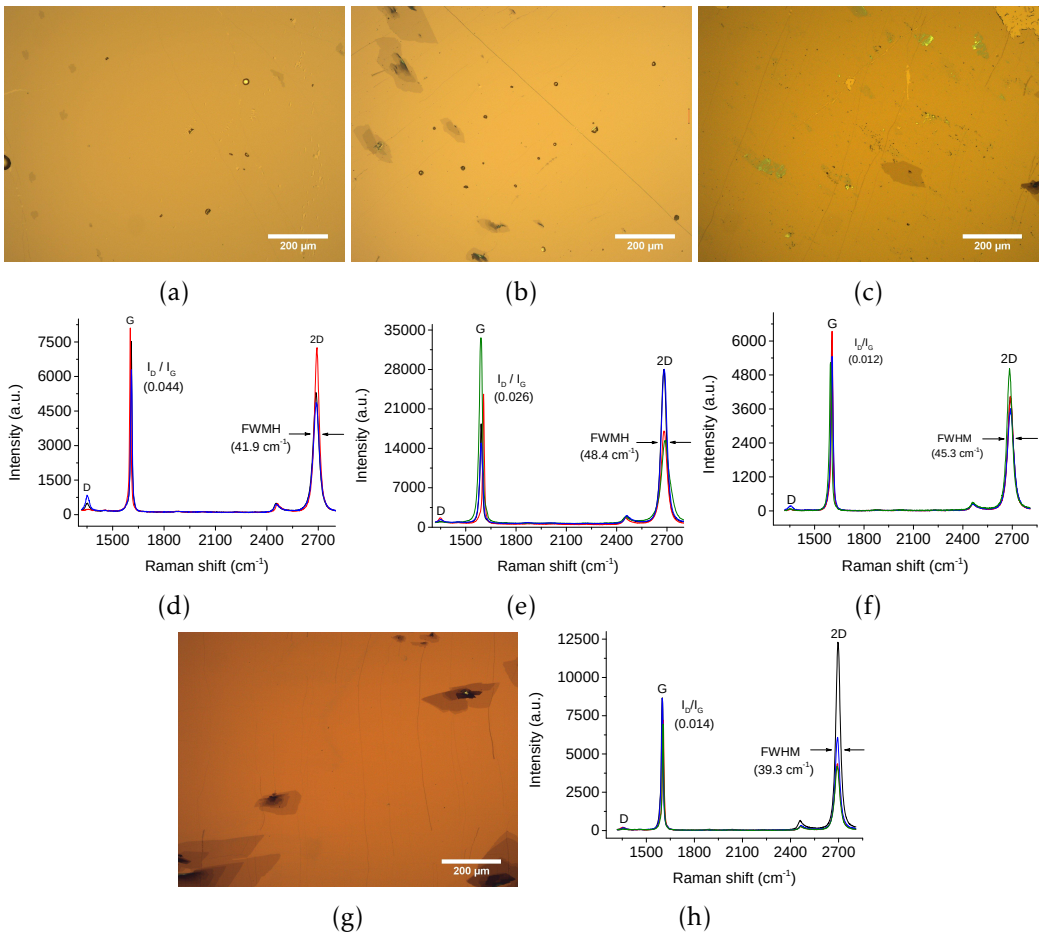

Figure 3.5: Optical microscopy images after a wet graphene transfer with (a) $NaNO_3$, (b) Na_2SO_4, (c) K_2SO_4 and (g) TMACl and their respective (d, e, f, h) Raman spectra measured in four different points.

in order to detach the PDMS and stack from the platinum foil. This auxiliary force tell us that the delamination is very slow and non-natural and thus, these electrolytes are not adequate for delaminating graphene. Regarding $Ce(SO_4)_2$, it was diluted in 0.2 M of H_2SO_4 because it did not dissolve well only in water. With it, the stack/PDMS did not separate at all from the Pt foil while at the same time cerium ion was precipitating around the cathode. Then, the wet-transfer was done for all these electrolytes but without success proving the assumed logic: when the dry-transfer is not a natural process the wet-transfer will not work.

These results show that not only the hydrogen bubbles are important to the delamination of the stack but also the type of cation that is attracted to the interface. Sodium, potassium, tetramethylammonium and tetraethylammonium ions appear to be helping further water intercalation through the interface (and therefore helping the delamination of the stack) while ammonia, hydrogen and cerium ions do not. In this matter, Na^+, K^+, TMA^+ and TEA^+ appear to reach the cathode without reacting, they intercalate between the platinum and the stack spreading them and helping the delamination. On

the contrary, $NH_4{}^+$ (eq. 3.1), H^+ (eq. 3.2) and Ce^{4+} (eq. 3.3) are reduced as soon as they reach the electrode (cathode) and are not helping the delamination at all. Although Ce^{4+} reduces to Ce^{3+}, this ion still will not intercalate in between graphene and platinum because it exceeds its solubility limit and starts to precipitate as $Ce_2(SO_4)_3$, not aiding the delamination.

$$2\,NH_4OH\,(aq) + 2\,e^- \longrightarrow 2\,NH_3\,(g) + H_2\,(g) + 2\,OH^-\,(aq) \tag{3.1}$$

$$2\,H^+\,(aq) + 2\,e^- \longrightarrow H_2\,(g) \tag{3.2}$$

$$Ce^{4+}\,(aq) + e^- \longrightarrow Ce^{3+}\,(aq) \tag{3.3}$$

In order to have a better overview on which cations work with the electrochemical delamination, a mechanism based on the electrochemical window (EW) of water is proposed. In this window, it is possible to clearly see a range between the potentials for water reduction and oxidation. Since the graphene is in the negative side (cathode) only the part where there are negative currents is relevant. Here, the reduction of water takes place and hydrogen bubbles are produced only when a potential more negative than the onset potential of this reaction (reduction point) is applied. Different pH values in the solution means that there are different concentrations of $[H^+]/[OH^-]$ ions available for the reaction, that will require different potentials (more or less) to start reacting. This relationship can be correlated with the Nernst equation that indicates the cell potential according to the pH of the solution, in this case being the potential to produce H_2 bubbles depending on the pH of the electrolyte used. For acidic solutions the reduction point is around 0 V, for neutral solutions around -0.4 V and for alkaline solutions around -0.8 V (see Appendix C for calculations). Figure 3.6 depicts that region of the water EW with all the cations involved. It is divided into two regions: the first (I) is where hydrogen bubbles are being produced after the reduction point (negative direction) and the second (II) where there are no water reduction (positive direction). The electrolytes that worked (with Na^+ and K^+) are far to the left from the reduction point and the ones that did not (with H^+, $NH_4{}^+$ and Ce^{4+}) are right at the border of it or far to the right from the reduction point. Meanwhile, TMA^+ and TEA^+ have a relatively low electroreductive reactivity, and are thus expected to intercalate between graphene and the Pt foils because they will not react.

To assure that graphene delamination is successful, it is imperative that the cations have a low electroreductive reactivity (like TMA^+ and TEA^+) or that they reduce at potentials more negative to the hydrogen evolution reaction (like Na^+ and K^+), which consequently means that is the water/hydrogen ion that is being reduced and not the cations. In other words, the reduction half-reaction needs to be outside of the EW so that the cations will not reduce, but the water will. For example, Na^+ has a reduction potential of -2.7 V and H_2O a reduction potential of -0.8 V (for alkaline solutions). Since the reduction of water to hydrogen occurs at more positive potentials, it will accept electrons

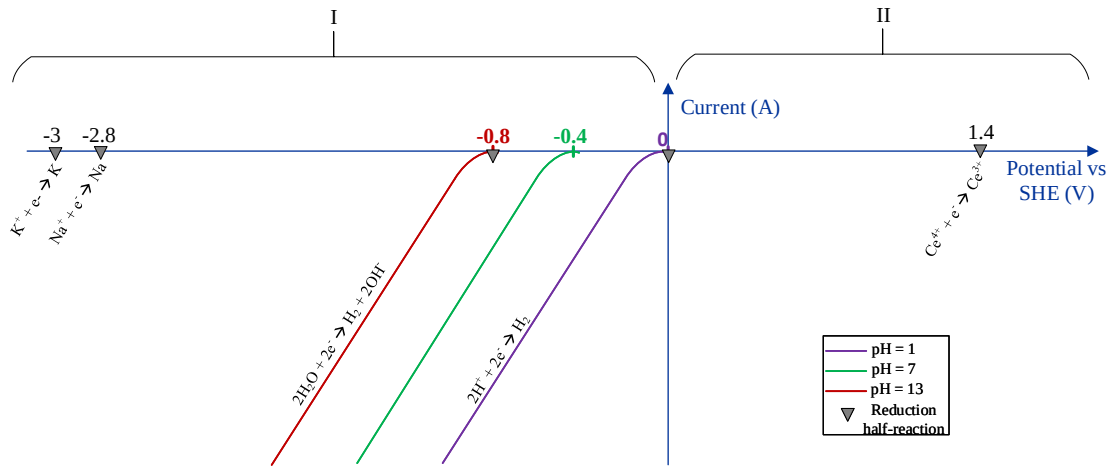

Figure 3.6: Zoom in of the reduction area in a water electrochemical window with the cations of the electrolytes used represented according to their reduction potential. The regions will shift according to the reduction point.

more easily and will reduce first. This will "block" Na^+ reduction, not reacting with the electrode and therefore helping the intercalation. In contrast, Ce^{4+} is at 1.4 V against 0.0 V (for acidic solutions) of H^+ which implies that cerium ion will react before the hydrogen ion. Moreover, as said before, Ce^{3+} will form a solid meaning that will not help the intercalation and thus the chosen electrolyte will not work. The same for H^+ from H_2SO_4 and HNO_3, that reduces at the same time as the water reduction and only contributes for more production of hydrogen bubbles and not for the intercalation.

Until now the hydrogen bubbles were considered a determining factor for the success of the electrochemical method, an assumption that in fact is revealed incorrect and at its best only accelerates graphene delamination. As a matter of fact, with H_2SO_4 and HNO_3 the H^+ is reduced to H_2 and therefore more hydrogen bubbles are being produced and the delamination still does not work. It is also important to emphasize that the cell potential was always set at -2.5 V (overpotential), being enough potential to overcome the various activation barriers and reduce the water. Furthermore, the mechanism used was a two-electrode setup, which does not fully control the exact values of the potentials. The values given in the EW (the calculated ones) are always vs standard hydrogen electrode (SHE) and thus the cell potential cannot be represented in the EW. The hydrogen bubbles produced follows different reactions depending on the pH of the solution, following the chemical eq. (2.1) for alkaline electrolytes, eq. (2.4) for acidic and a combination of the two for neutral pH.

3.3.2 Sample as anode

To obtain process optimization it is important to find other ions that also intercalate between the interface of platinum/graphene and drive the delamination forward, as good as Na^+ does. In the following experiments, the polarity has been changed to attract

negatively charged anions to a positively charged anode. The electrolytes used were some of the ones used in the cathode configuration with a few more added: sodium chloride (NaCl) and sodium sulfite (Na_2SO_3). Figure 3.7 shows them with the respective anion that is being attracted to the interface.

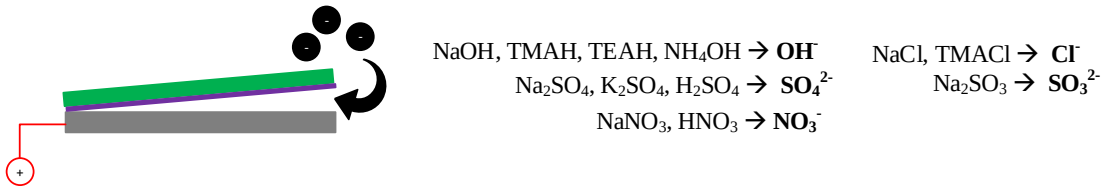

Figure 3.7: Anions of an electrolyte being attracted by the electrode (anode). The anions of each electrolyte are marked in black.

Electrolytes such as $NaNO_3$, HNO_3, Na_2SO_4, K_2SO_4 and H_2SO_4 worked in the dry--transfer requiring a soft pull in the PDMS to help the delamination. Once again, there is some evidence that the type of ion that is in the interface (in this case nitrate and sulfate ion) matters to the delamination of the stack since electrolytes that did not work before in the cathode setup (HNO_3 and H_2SO_4) are now working. Nevertheless, it is important to note that it was still a pull in the PDMS (soft or hard) predicting a hard wet-transfer. Indeed, the wet-transfer worked but it had to be assisted by a tweezer (by pulling the corners and the parts that got stuck), contributing to a long non-natural delamination and the probability of defecting the graphene. Additionally, the voltage had to be increased from 2.5 V to 4 V in order to start peeling the corners of the stack. The same results are produced with TMACl and NaCl. Figure 3.8 shows the optical microscope images and the Raman characterization for each wet-transfer. A uniform and wrinkled graphene was obtained with a presence of some cracks probably due the harsh handling while doing the delamination. The Raman spectra reveals large strain variations for some of them (not for K_2SO_4 and TMACl) indicated by the high FWHM although it shows a low I_D/I_G peak ratio (< 6%). A particular note to 3.8f that shows a highly defective graphene (I_D/I_G = 51%) although the optical microscopy image does not show major defects. This example perfectly demonstrates why is so important to combine different characterization techniques when studying graphene. The high D peak was originated during the transfer probably due the severe handling (pulling the corners, etc.), stressing the importance of a free/minimal handling during graphene transfer.

The electrolytes that did not work were NaOH, NH_4OH, TMAH and TEAH. Likewise, it is believed that as soon as the hydroxide ion reaches the electrode (anode) it oxidizes into O_2 according to eq. (2.2) not contributing to the delamination. This does not happen for the electrolytes with $SO_4{}^{2-}$ and $NO_3{}^{-}$ ions. The water EW logic was again applied, this time for water oxidation since graphene is connected to the positive side (anode) and the relevant current values are now positive. In this case, oxygen bubbles are produced instead of hydrogen at the adequate potential (oxidation point). For the same reasons explained before, the oxidation potential will depend on the pH of the electrolyte. For

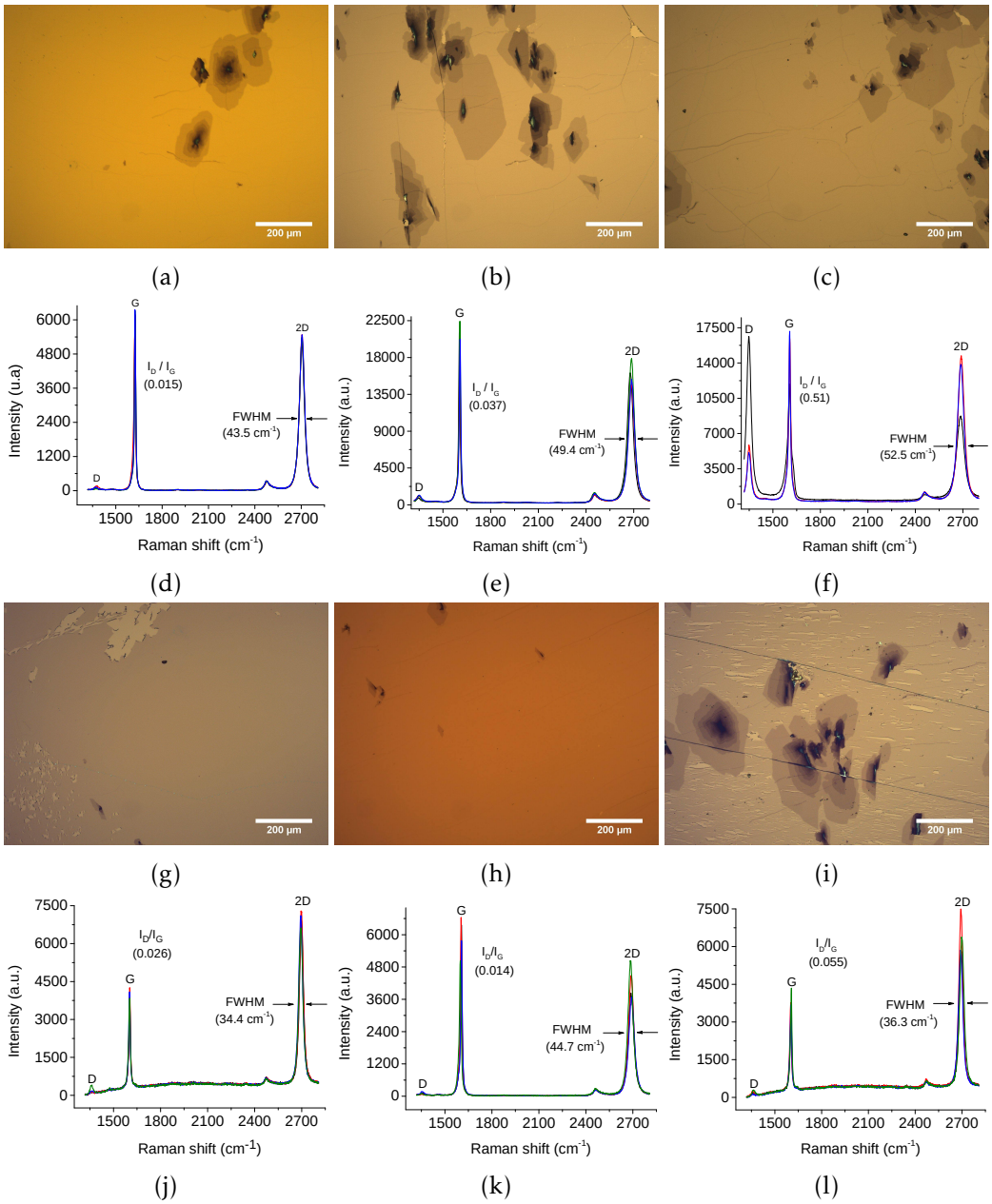

Figure 3.8: Optical microscopy images after a wet graphene transfer with (a) HNO_3, (b) $NaNO_3$, (c) Na_2SO_4, (g) K_2SO_4, (h) TMACl and (i) NaCl and their respective (d, e, f, j, k, l) Raman spectra measured in four different points.

acidic solutions the oxidation point is around 1.2 V, for neutral solutions around 0.8 V and for alkaline solutions around 0.4 V (see Appendix C for calculations). Figure 3.9 depicts that region of the water EW with all the anions involved. Similarly, it is divided into two regions: the first (I) where there is no water oxidation (negative direction) and the second (II) where after the oxidation point oxygen bubbles are being produced (positive direction). The electrolytes that worked have their anions (SO_4^{2-} and Cl^-) to the right from the oxidation point and the ones that did not (OH^-) are again at the border of it. A note to NO_3^- that is already in its highest oxidation state (N(+V)) so cannot oxidize further, helping the intercalation through the interface.

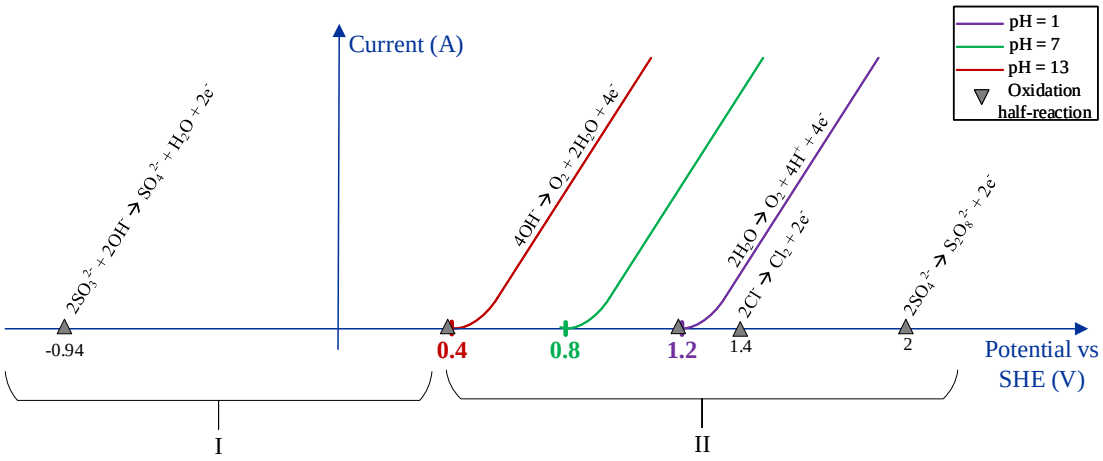

Figure 3.9: Zoom in of the oxidation area in a water electrochemical window with the anions of the electrolytes used represented according to their oxidation potential. The regions will shift according to the oxidation point.

For the case of Na_2SO_3, the experiment worked as Figure 3.10 depicts. The optical microsopy image shows a good transfer despite a few cracks while the Raman spectra reveals a non-defective ($I_D/I_G < 5\%$) and smooth graphene (not high FWHM). However, according to the EW, the SO_3^{2-} ion has a oxidation potential inside the window (region I) and not outside so, it should not work. Surprisingly, it works as good with sulfate ion. The successful transfer can be explained by the electrochemical reaction of SO_3^{2-} ion that oxidizes to SO_4^{2-} at -0.94 V. It will oxidize first than the water because has a more negative potential and thus give away electrons more easily. Then, after oxidation it stays as SO_4^{2-} which is the anion that pushes the intercalation forward and allows graphene to delaminate as now it is outside the EW, in zone II.

All these experiments, underline again that the ion that is attracted to the interface is crucial, and not the hydrogen bubbles. In fact, no hydrogen bubbles are produced in this setup and the delamination still works. Instead of hydrogen, oxygen bubbles are produced due the water oxidation but yet, they reveal unrelated with graphene delamination since the non-reaction of the anion is what counts to graphene delamination. Nevertheless, graphene can be degraded due the oxygen bubbles formed and electrical measurements should be performed to better confirm that. It is also important to note

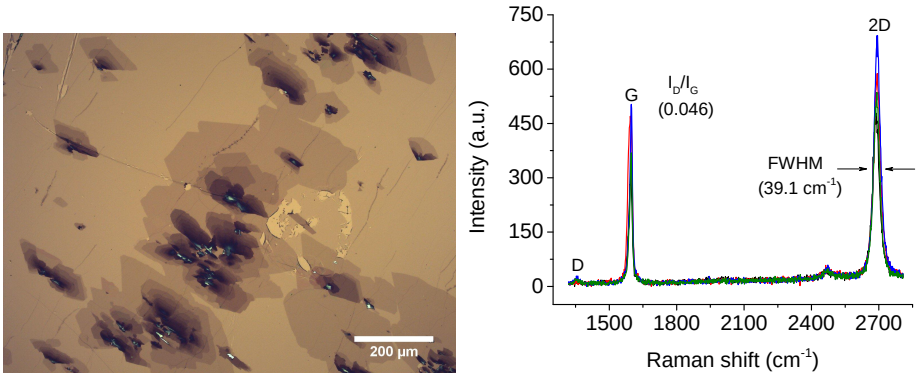

(a) (b)

Figure 3.10: (a) Optical microscopy image after a wet graphene transfer with Na_2SO_3 and its respective (b) Raman spectra measured in four different points.

that the cell potential was always set at 4 V (overpotential), being enough potential to overcome the various activation barriers and oxidize the water. Moreover, the mechanism used was a two-electrode setup, which does not fully control the exact values of the potentials. The values given in the EW (the calculated ones) are always vs SHE and thus the cell potential cannot be represented in the EW. The oxygen bubbles produced follows different reactions depending on the pH of the solution, following the chemical eq. (2.2) for alkaline electrolytes, eq. (2.5) for acidic and a combination of the two for neutral pH.

Table 3.1 summarizes the results for every transfer in each setup. An electrolyte should hence be chosen taking in account its redox potential and that its charged species have to withstand the electrochemical process (i.e., not being neutralized or precipitated) so it can assist graphene delamination. Yet, for some unknown reason, ions/molecules are always attracted between graphene and platinum. As matter of fact, graphene delamination can work without electrolysis, i.e. without needing a potential. By only using the electrolyte without any current, the redox reactions of the ions are limited/eliminated and therefore they can all contribute to intercalation. However, graphene takes a long time to delaminate and the process can be accelerated via a potential where cations/anions are attracted and that was what this thesis discussed. After all these experiments, the cathode setup gave better transfer results than the anode setup despite the mechanism behind the delamination (i.e., ion being attracted cannot react with the electrode) was the same. This can be addressed in the future by taking the doping of the graphene layer into account since the polymer used (PC) is responsible for p-doping graphene [76].

Table 3.1: Electrolyte study results summary. Legend: (✓) worked, (✕) did not work, (±) non-natural delamination, (—) not tried.

	Cathode setup		Anode Setup		
Electrolyte	Dry-transfer	Wet-transfer	Dry-transfer	Wet-transfer	pH
NaOH	✓	✓	✕	✕	13.3
TMAH	✓	✓	✕	✕	13
TEAH	✓	✓	✕	✕	13
NH_4OH	±	✕	✕	✕	11.3
$NaNO_3$	✓	✓	✓	±	7
Na_2SO_4	✓	✓	✓	±	7
Na_2SO_3	—	—	✓	±	7
K_2SO_4	✓	✓	✓	±	7
TMACl	✓	✓	✓	±	7
NaCl	—	—	✓	±	7
HNO_3	±	✕	✓	±	0.7
H_2SO_4	±	✕	✓	±	0.4
$Ce(SO_4)_2$	✕	✕	—	—	0.4

3.4 Graphene's adhesion to HSQ

One parameter that is crucial to a successful transfer is graphene's adhesion to the substrates. For example, in the case of the direct transfer it is important that the adhesion between target substrate/graphene surpasses the adhesion between the growth substrate/-graphene so the graphene can be easily transferred. Graphene has a low reactivity so most adhesion is caused by Van der Waals forces [77] and a good/high adhesion is described when graphene follows the morphology of the substrate. As often repeated, this limitation is one of the main reasons for a unsuccessful transfer in the electrochemical method and therefore a critical aspect to take in account. Moreover, in graphene direct transfer for example, the Si/SiO_2 substrate (pretreated with a perfluorodecyltrichlorosilane (FDTS) layer to become hydrophobic) has the inconvenient of doping the graphene, not being an ideal target substrate.

Hydrogen silsesquioxane (HSQ) is a low dielectric constant material that changes its structure according to the curing temperature, it has a cage structure before curing and a network structure after curing where its properties depend strongly on the curing process. Its particular use with graphene comes from the fact that it behaves like a polymer before curing (graphene has proven to have a high adhesion with some polymers [47, 78]) and transforms partially into SiO_2 after curing [79]. Thus, HSQ is ideal to use as a target substrate because it can planarize the surface and can easily be spin-coated, perhaps making a good adhesion with graphene and then be transformed into SiO_2. Furthermore, it does not dope the graphene in comparison with the FDTS-treated substrates used before and it is also hydrophobic, a parameter needed in order to do a direct transfer.

To test graphene's adhesion to HSQ a standard wet electrochemical method is used.

Figure 3.11a shows the microscope image before removing the polymer (PC). After dissolving the polymer with its respective solvent (see Appendix B) it was noticed that the majority of the graphene sheet had already delaminated. Figure 3.11b confirms that, where the zones that only have graphene are the zones that still have PC, which were zones that the solvent did not have time to remove. This means that the HSQ, being still a polymer, also gets removed by the same solvent used to remove PC [80] and since graphene is on top of HSQ, all the structure is removed. The curing process is then needed so HSQ can be transformed into SiO_2 so later-on PC is the only material removed by the solvent. However, PC cannot undertake a curing process because if it goes through such a procedure, it hardens and it is almost impossible to remove by its solvent (Figure 3.11c).

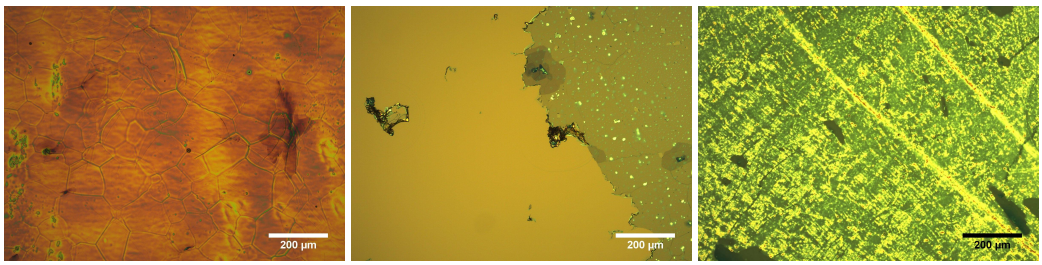

(a) (b) (c)

Figure 3.11: Optical microscopy image after a wet graphene transfer with HSQ as target substrate (a) before polymer removal, (b) after polymer removal and (c) after annealing and polymer removal.

Hence, the support material had to be changed to one that ideally could support high temperatures and still get removed afterwards. The chosen material was poly-methyl methacrylate (PMMA) because it is actually removed by an annealing process at 400 °C (see Appendix B). The intention is now to transfer graphene by a wet-transfer to a standard target substrate spin-coated with HSQ (Si/SiO_2/HSQ/graphene/PMMA), cure the sample and at the same time remove the polymer ($Si/SiO_2/SiO_2$/graphene). Figure 3.12 shows the sample before and after curing. The graphene maintained in the target with no cracks, few wrinkles, not much polymer contamination and with no additional damage. The Raman spectra shows a very high-quality graphene with an I_D/I_G ratio inferior to 1% although not entirely flat as the high FWHM value points out.

To make sure and to check how much of the HSQ suffered the transformation after the curing step an water contact angle test should be done in the future since HSQ as polymer is hydrophobic while SiO_2 is hydrophilic. Furthermore, HSQ could also follow another approach such as a support layer to stack 2D materials.

3.5 Direct Transfer - a solution?

TMAH, TMACl and TEAH used in cathode setup were the electrolytes responsible for the best graphene transfer which do not have sodium contamination. Between them, TEAH is the most promising option because is less toxic than the others and therefore user

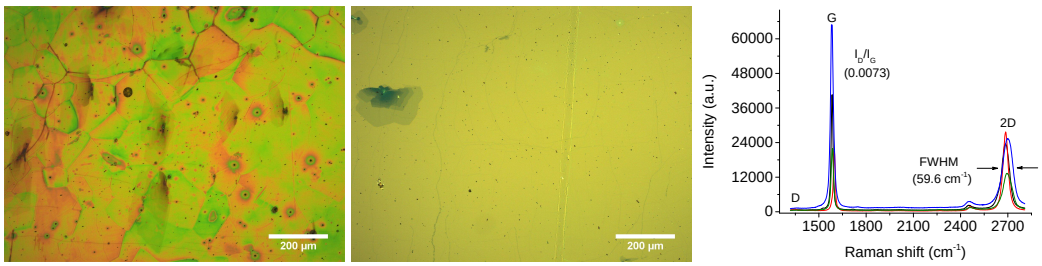

(a) (b) (c)

Figure 3.12: Optical microscopy images after a wet graphene transfer with HSQ as target substrate (a) before and (b) after polymer removal and its respective (c) Raman spectra measured in four different points.

friendly. With that in mind, a direct graphene transfer was tried with the hydrophobic FDTS target substrate. As expected the transfer was successful as Figure 3.13 depicts. No additional damage can be seen and a high-quality graphene (with a very low I_D/I_G peak ratio) with a smooth surface (small FWHM) is present, as Raman spectra shows. The sodium contamination is finally avoided maintaining a very good quality transfer.

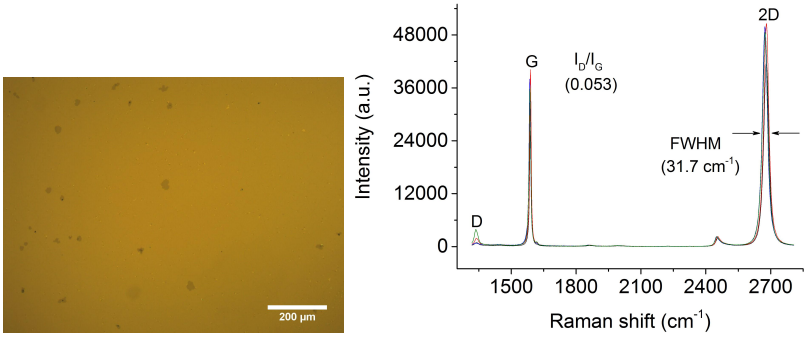

(a) (b)

Figure 3.13: Optical microscopy image after a direct graphene transfer with (a) TMAH, (b) TEAH and (c) TMACl and their respective (d,e,f) Raman spectra measured in four different points.

The problem that is still in hand is the doping provoked by the FDTS target. Although HSQ proved to have good adhesion with graphene and avoids the doping it does not seem to be a good candidate as target substrate because of its post bad quality SiO_2 that can introduce uncontrolled charges in the graphene sheet. Additionality, HSQ reacts when in contact with alkaline hydroxide groups [81] making a narrow selection for the electrolytes that can be used. Nonetheless, a direct transfer with TMACl, for example, and HSQ as target substrate can be done to conclude the study and verify that if in fact it will be a good target substrate contender.

Overall, the direct transfer is preferable over the others techniques not only because of the uniform high-quality transferred graphene with no cracks and a lot less multi-layers (due the growing conditions) but mostly because of the successful transfer without polymer contamination. Although it is an expensive path, with the continuing optimization of this method, the graphene transfer issue is a step closer to be solved.

Chapter 4

Conclusion and Future Perspectives

Electrochemical delamination is the preferable graphene transfer technique due its non-destructive behaviour towards the growing substrate, being able to be recycled and reused again. The direct transfer, which working principle is based on the electrochemical delamination, holds the promise of achieving a scalable transfer method for high-quality graphene, a requirement needed for producing industrial graphene for many applications. However, it is still an expensive technique due to the growth substrate used and has some issues that this thesis engaged to solve: the sodium contamination and the doping in graphene caused, respectively, by the electrolyte and the target substrate already used.

Sodium hydroxide is the frequently electrolyte used in electrochemical delamination that concedes a very good and uniform transferred graphene. However, is the responsible for the sodium contamination unwanted in graphene. Until now, the amount of hydrogen bubbles was considered by the literature a determining factor for graphene delamination. This study contradicts it by saying that it is not the hydrogen bubbles that help graphene delaminate but rather the charged species from the electrolyte. In fact, the hydrogen bubbles do not influence at all the delamination (or at its best only accelerates it), being only a product of water reduction. What does really matter are the ions (cations and anions) from the electrolyte, as the cathodic and anodic studies from the electrolyte study demonstrates. It is imperative that the ions "survive" the electrochemical process (i.e., by not being neutralized or precipitated) so they can intercalate between the interface of graphene and the growth substrate and push the delamination forward. Additionally, based on the proposed mechanism of the electrochemical window of water, this work concludes that any ion outside this window (more negative values when is water reduction in cathode setup and more positive values when is water oxidation in anode setup) or ions that have a relatively low electroreductive reactivity will help in graphene delamination. TEAH for example is one of the electrolytes that can replace NaOH maintaining a high-quality and undamaged transferred graphene while simultaneously avoiding the sodium contamination.

Graphene's adhesion, is perhaps one of the most difficult challenges in graphene transfer. Whatever the method used in the transfer, a good adhesion with the target substrate is fundamental. Otherwise, the transfer will always be unsuccessful. Another problem to be solved is the doping that the hydrophobic Si/SiO_2 substrate used in direct transfer caused in graphene. HSQ emerged as a good solution because it can planarize the surface, it is hydrophobic so it can repel water and avoid intercalation and it does

not dope the graphene comparing with the FDTS substrate used. It has a good adhesion to graphene, as this study reveals, but unfortunately transforms into low quality SiO_2 after curing and can introduce uncontrolled charges in the graphene sheet, not being an ideally target substrate.

The next step would be continuing the studies in order to fully confirm the new findings. Firstly, the doping that graphene layer has should be taken in account by electrical characterization. That could explain why cations work better than anions in the electrochemical delamination since the polymer used (PC) is responsible for a p-doping in the graphene. Secondly, a direct transfer with HSQ should be done with a non-alkaline electrolyte that contains hydroxide groups (like TMACl) to confirm if it is a promising target substrate as well contact angle tests to verify if HSQ is in fact transforming into SiO_2 (and how much is suffering the transformation). Moreover, new approaches that do not consider HSQ as target substrate could be taken, such as considering it as a support layer and stack 2D materials with it. Finally, the home-made bonder should be improved to support vacuum so it is possible to completely avoid trapped molecules between graphene and the target material in the direct transfer.

Overall, the preset ideas of this work were accomplished and part of the full problem was solved. With continuously optimized growth mechanism for single-layer graphene the lack of a suitable transfer process is without doubts the main obstacle for upscaling towards industrial graphene. Direct transfer is probably one of the most promising methods that can fill this gap and shine towards an exciting future for graphene. With the insight of the mechanism studied by this thesis, now it is possible to select electrolytes that would not contain alkali elements and therefore pose no contamination risk for CMOS.

Bibliography

[1] R. Mas-Ballesté, C. Gómez-Navarro, J. Gómez-Herrero, and F. Zamora. "2D materials: to graphene and beyond." In: *Nanoscale* 3.1 (2011), pp. 20–30. ISSN: 2040-3364. DOI: 10.1039/c0nr00323a.

[2] M. Aliofkhazraei, N. Ali, W. I. Milne, C. S. Ozkan, S. Mitura, and L. J. Gervasoni. *Graphene Science Handbook. Size-Dependent Properties*. Taylor & Francis Group, 2016, p. 494. ISBN: 9781466591363.

[3] A. H. Castro Neto, F. Guinea, N. M. R. Peres, K. S. Novoselov, and A. K. Geim. "The electronic properties of graphene." In: *Reviews of Modern Physics* 81.1 (2009), pp. 109–162. ISSN: 00346861. DOI: 10.1103/RevModPhys.81.109.

[4] P. R. Wallace. "The band theory of graphite." In: *Physical Review* 71.9 (1947), pp. 622–634. ISSN: 0031899X. DOI: 10.1103/PhysRev.71.622.

[5] L. D. Landau. "On the theory of phase transitions." In: *Zh. Eks. Teor. Fiz.* 7.1937 (1937), pp. 19–32. ISSN: 0028-0836. DOI: 10.1038/138840a0.

[6] D Mermint. "Crystalline Order in Two Dimensions." In: *Physical Review* 176.1 (1968).

[7] K. S. Novoselov, A. K. Geim, S. V. Morozov, D Jiang, Y Zhang, S. V. Dubonos, I. V. Grigorieva, and A. A. Firsov. "Electric Field Effect in Atomically Thin Carbon Films." In: *Science* 306.5696 (2004), pp. 666–669. ISSN: 0036-8075. DOI: 10.1126/science.1102896.

[8] K. S. Novoselov, D Jiang, F Schedin, T. J. Booth, V. V. Khotkevich, S. V. Morozov, and A. K. Geim. "Two-dimensional atomic crystals." In: *PNAS* 102.30 (2005), pp. 10451–10453. ISSN: 0027-8424. DOI: 10.1073/pnas.0502848102.

[9] Y. B. Zhang, Y. W. Tan, H. L. Stormer, and P. Kim. "Experimental observation of the quantum Hall effect and Berry's phase in graphene." In: *Nature* 438.7065 (2005), pp. 201–204. ISSN: 0028-0836. DOI: 10.1038/nature04235.

[10] K. S. Novoselov, A. K. Geim, S. V. Morozov, D Jiang, M. I. Katsnelson, I. V. Grigorieva, S. V. Dubonos, and A. A. Firsov. "Two-dimensional gas of massless Dirac fermions in graphene." In: *Nature* 438.7065 (2005), pp. 197–200. ISSN: 0028-0836. DOI: 10.1038/nature04233.

[11] Nobleprize.org. *The 2010 Nobel Prize in Physics*. URL: http://www.nobelprize.org/nobel{_}prizes/physics/laureates/2010/press.html (visited on 05/14/2017).

[12] W. Choi, I. Lahiri, R. Seelaboyina, and Y. S. Kang. "Synthesis of Graphene and Its Applications: A Review." In: *Critical Reviews in Solid State and Materials Sciences* 35.1 (2010), pp. 52–71. ISSN: 1040-8436. DOI: 10.1080/10408430903505036.

[13] A. Hirsch. "The era of carbon allotropes." In: *Nature Materials* 9.11 (2010), pp. 868–871. ISSN: 1476-1122. DOI: 10.1038/nmat2885.

[14] S. Fujii and T. Enoki. "Nanographene and Graphene Edges: Electronic Structure and Nanofabrication." In: *Accounts of Chemical research* 46.10 (2012), pp. 2202–2210.

[15] R. R. Haering. "Band Structure of Rhombohedral Graphite." In: *Canadian Journal of Physics* 36 (1958), p. 352. ISSN: 0008-4204. DOI: 10.1007/978-3-642-13884-3_6.

[16] A. Geim and K. Novoselov. "The Rise of Graphene." In: *Nature materials* (2007), pp. 183–191. ISSN: 1476-1122. DOI: 10.1038/nmat1849.

[17] A. K. Geim and P. Kim. "Carbon Wonderland." In: *Scientific American* 298.4 (2008), pp. 90–97. ISSN: 0036-8733. DOI: 10.1038/scientificamerican0408-90.

[18] M. S. A. Bhuyan, M. N. Uddin, M. M. Islam, F. A. Bipasha, and S. S. Hossain. "Synthesis of graphene." In: *International Nano Letters* 6.2 (2016), pp. 65–83. ISSN: 2008-9295. DOI: 10.1007/s40089-015-0176-1.

[19] G. Peschel. *Carbon - Carbon bonds: Hybridization*. 2011. URL: http://www.physik.fu-berlin.de/einrichtungen/ag/ag-reich/lehre/Archiv/ss2011/docs/Gina{_}Peschel-Handout.pdf.

[20] J. H. Warner, F. Schäffel, A. Bachmatiuk, and M. Rümmeli. *Graphene-Fundamentals and Emergent Applications*. 2013, p. 437. ISBN: 9780123945938.

[21] E. Z. *State and briefly describe the main modes of hybridization that carbon undergoes when it forms nearly 10 million compounds?* 2015. URL: https://socratic.org/questions/state-and-briefly-describe-the-main-modes-of-hybridization-that-carbon-undergoes (visited on 05/10/2017).

[22] P. Avouris. "Graphene: Electronic and photonic properties and devices." In: *Nano Letters* 10.11 (2010), pp. 4285–4294. ISSN: 15306984. DOI: 10.1021/nl102824h.

[23] M. S. Dresselhaus, G. Dresselhaus, and R. Saito. "Physics of carbon nanotubes." In: *Carbon* 33.7 (1995), pp. 883–891. ISSN: 00086223. DOI: 10.1016/0008-6223(95)00017-8.

[24] S. V. Morozov, K. S. Novoselov, M. I. Katsnelson, F. Schedin, D. C. Elias, J. A. Jaszczak, and A. K. Geim. "Giant intrinsic carrier mobilities in graphene and its bilayer." In: *Physical Review Letters* 100.1 (2008), pp. 11–14. ISSN: 00319007. DOI: 10.1103/PhysRevLett.100.016602.

[25] K. Verguts, N. Vrancken, B. F. Vermeulen, C. Huyghebaert, H. Terryn, S. Brems, and S. De Gendt. "Single-Layer Graphene Synthesis on a Al2O3(0001)/Cu(111) Template Using Chemical Vapor Deposition." In: *ECS Journal of Solid State Science and Technology* 5.11 (2016), Q3060–Q3066. ISSN: 2162-8769. DOI: 10.1149/2.0121611jss.

[26] E. Suárez Morell, M. Pacheco, L. Chico, and L. Brey. "Electronic properties of twisted trilayer graphene." In: *Physical Review B - Condensed Matter and Materials Physics* 87.12 (2013), pp. 1–7. ISSN: 10980121. DOI: 10.1103/PhysRevB.87.125414.

[27] A. Yacoby. "Graphene: Tri and tri again." In: *Nature Physics* 7.12 (2011), pp. 925–926. ISSN: 1745-2473. DOI: 10.1038/nphys2166.

[28] Y. Zhang, T.-T. Tang, C. Girit, Z. Hao, M. C. Martin, A. Zettl, M. F. Crommie, Y. R. Shen, and F. Wang. "Direct observation of a widely tunable bandgap in bilayer graphene." In: *Nature* 459.7248 (2009), pp. 820–823. ISSN: 0028-0836. DOI: 10.1038/nature08105.

[29] S. Salimian and M. E. Azim Araghi. "Manual turbostratic stacked graphene transistor: A study on electrical properties and device potential." In: *Diamond and Related Materials* 68 (2016), pp. 28–36. ISSN: 09259635. DOI: 10.1016/j.diamond.2016.05.012.

[30] M. F. Craciun, S. Russo, M. Yamamoto, and S. Tarucha. "Tuneable electronic properties in graphene." In: *Nano Today* 6.1 (2011), pp. 42–60. ISSN: 17480132. DOI: 10.1016/j.nantod.2010.12.001.

[31] M. Freitag. "Graphene: Trilayers unravelled." In: *Nature Physics* 7.8 (2011), pp. 596–597. ISSN: 1745-2473. DOI: 10.1038/nphys2032.

[32] D. A. C. Brownson and C. E. Banks. *The Handbook of Graphene Electrochemistry*. Springer, 2014, p. 201. ISBN: 9781447164722. DOI: 10.1007/978-1-4471-6428-9.

[33] K. S. Novoselov, Z. Jiang, Y. Zhang, S. V. Morozov, H. L. Stormer, U. Zeitler, J. C. Maan, G. S. Boebinger, P. Kim, and A. K. Geim. "Room-Temperature Quantum Hall Effect in Graphene." In: *Science* 315.5817 (2007), pp. 1379–1379. ISSN: 0036-8075. DOI: 10.1126/science.1137201.

[34] L. Banszerus, M. Schmitz, S. Engels, J. Dauber, M. Oellers, F. Haupt, K. Watanabe, T. Taniguchi, B. Beschoten, and C. Stampfer. "Ultrahigh-mobility graphene devices from chemical vapor deposition on reusable copper." In: *Science Advances* 1.6 (2015), e1500222–e1500222. ISSN: 2375-2548. DOI: 10.1126/sciadv.1500222.

[35] S. Ghosh, I. Calizo, D. Teweldebrhan, E. P. Pokatilov, D. L. Nika, A. A. Balandin, W. Bao, F. Miao, and C. N. Lau. "Extremely high thermal conductivity of graphene: Prospects for thermal management applications in nanoelectronic circuits." In: *Applied Physics Letters* 92.15 (2008), pp. 1–4. ISSN: 00036951. DOI: 10.1063/1.2907977.

[36] C. Lee, X. Wei, J. W. Kysar, and J. Hone. "Measurement of the Elastic Properties and Intrinsic Strength of Monolayer Graphene." In: *Science* 321.5887 (2008), pp. 385–388. ISSN: 0036-8075. DOI: 10.1126/science.1157996.

[37] Z. Xu and C. Gao. "Graphene fiber: A new trend in carbon fibers." In: *Materials Today* 18.9 (2015), pp. 480–492. ISSN: 18734103. DOI: 10.1016/j.mattod.2015.06.009.

[38] F. Schwierz. "Graphene transistors." In: *Nature Nanotechnology* 5.7 (2010), pp. 487–496. ISSN: 1748-3387. DOI: 10.1038/nnano.2010.89.

[39] L. Liao and X. Duan. "Graphene for radio frequency electronics." In: *Materials Today* 15.7-8 (2012), pp. 328–338. ISSN: 13697021. DOI: 10.1016/S1369-7021(12)70138-4.

[40] L. Banszerus, M. Schmitz, S. Engels, M. Goldsche, K. Watanabe, T. Taniguchi, B. Beschoten, and C. Stampfer. "Ballistic Transport Exceeding 28 μm in CVD Grown Graphene." In: *Nano Letters* 16.2 (2016), pp. 1387–1391. ISSN: 15306992. DOI: 10.1021/acs.nanolett.5b04840. eprint: 1511.08601.

[41] S. K. Banerjee, L. F. Register, E. Tutuc, D. Basu, S. Kim, D. Reddy, and A. H. MacDonald. "Graphene for CMOS and beyond CMOS applications." In: *IEEE Xplore* 98.12 (2010), pp. 2032–2046. ISSN: 00189219. DOI: 10.1109/JPROC.2010.2064151.

[42] L. Britnell, R. V. Gorbachev, R. Jalil, B. D. Belle, F. Schedin, M. I. Katsnelson, L. Eaves, S. V. Morozov, N. M. R. Peres, J. Leist, A. K. Geim, K. S. Novoselov, and L. A. Ponomarenko. "Field-effect tunneling transistor based on vertical graphene heterostructures." In: *Science* 947.2012 (2011). ISSN: 0036-8075. DOI: 10.1126/science.1218461.

[43] H. Yang, J. Heo, S. Park, H. J. Song, D. H. Seo, K.-e. Byun, P. Kim, I. Yoo, H.-j. Chung, and K. Kim. "Graphene Barristor , a Triode Device with a Gate-Controlled Schottky Barrier." In: *Science* 336.Cvd (2012), pp. 1140–1143.

[44] P. Pasanen, M. Voutilainen, M. Helle, X. Song, and P. J. Hakonen. "Graphene for future electronics." In: *Physica Scripta* T146 (2012), p. 014025. ISSN: 0031-8949. DOI: 10.1088/0031-8949/2012/T146/014025.

[45] J. D. Fowler, M. J. Allen, V. C. Tung, Y. Yang, R. B. Kaner, and B. H. Weiller. "Practical chemical sensors from chemically derived graphene." In: *ACS Nano* 3.2 (2009), pp. 301–306. ISSN: 19360851. DOI: 10.1021/nn800593m.

[46] Q. Zheng, Z. Li, J. Yang, and J. K. Kim. "Graphene oxide-based transparent conductive films." In: *Progress in Materials Science* 64.March (2014), pp. 200–247. ISSN: 00796425. DOI: 10.1016/j.pmatsci.2014.03.004.

[47] S. Bae, H. Kim, Y. Lee, X. Xu, J.-S. Park, Y. Zheng, J. Balakrishnan, T. Lei, H. Ri Kim, Y. I. Song, Y.-J. Kim, K. S. Kim, B. Özyilmaz, J.-H. Ahn, B. H. Hong, and S. Iijima. "Roll-to-roll production of 30-inch graphene films for transparent electrodes." In: *Nature Nanotechnology* 5.8 (2010), pp. 574–578. ISSN: 1748-3387. DOI: 10.1038/nnano.2010.132.

[48] V. C. Tung, L. M. Chen, M. J. Allen, J. K. Wassei, K Nelson, R. B. Kaner, and Y Yang. "Low-Temperature Solution Processing of Graphene- Carbon Nanotube Hybrid Materials for High-Performance Transparent Conductors." In: *Nano Lett.* 9.5 (2009), p. 2513. ISSN: 1530-6984. DOI: 10.1021/nl9001525.

[49] B. Luo, S. Liu, and L. Zhi. "Chemical approaches toward graphene-based nanomaterials and their applications in energy-related areas." In: *Small* 8.5 (2012), pp. 630–646. ISSN: 16136810. DOI: 10.1002/smll.201101396.

[50] Q. Ke and J. Wang. "Graphene-based materials for supercapacitor electrodes – A review." In: *Journal of Materiomics* 2.1 (2016), pp. 37–54. ISSN: 23528478. DOI: 10.1016/j.jmat.2016.01.001.

[51] G. Wang, X. Shen, J. Yao, and J. Park. "Graphene nanosheets for enhanced lithium storage in lithium ion batteries." In: *Carbon* 47.8 (2009), pp. 2049–2053. ISSN: 00086223. DOI: 10.1016/j.carbon.2009.03.053.

[52] H. J. Choi, S. M. Jung, J. M. Seo, D. W. Chang, L. Dai, and J. B. Baek. "Graphene for energy conversion and storage in fuel cells and supercapacitors." In: *Nano Energy* 1.4 (2012), pp. 534–551. ISSN: 22112855. DOI: 10.1016/j.nanoen.2012.05.001.

[53] X. F. Lin, Z. Y. Zhang, Z. K. Yuan, J. Li, X. F. Xiao, W. Hong, X. D. Chen, and D. S. Yu. "Graphene-based materials for polymer solar cells." In: *Chinese Chemical Letters* 27.8 (2016), pp. 1259–1270. ISSN: 10018417. DOI: 10.1016/j.cclet.2016.06.041.

[54] S. Stankovich, D. A. Dikin, G. H. B. Dommett, K. M. Kohlhaas, E. J. Zimney, E. A. Stach, R. D. Piner, S. T. Nguyen, and R. S. Ruoff. "Graphene-based composite materials." In: *Nature* 442.7100 (2006), pp. 282–286. ISSN: 0028-0836. DOI: 10.1038/nature04969.

[55] B. Chen, H. Huang, X. Ma, L. Huang, Z. Zhang, and L.-M. Peng. "How good can CVD-grown monolayer graphene be?" In: *Nanoscale* 6.24 (2014), pp. 15255–61. ISSN: 2040-3372. DOI: 10.1039/c4nr05664g.

[56] L. Gao, W. Ren, H. Xu, L. Jin, Z. Wang, T. Ma, L.-P. Ma, Z. Zhang, Q. Fu, L.-M. Peng, X. Bao, and H.-M. Cheng. "Repeated growth and bubbling transfer of graphene with millimetre-size single-crystal grains using platinum." In: *Nature Communications* 3 (2012), p. 699. ISSN: 2041-1723. DOI: 10.1038/ncomms1702.

[57] S. Gorantla, A. Bachmatiuk, J. Hwang, H. a. Alsalman, J. Y. Kwak, T. Seyller, J. Eckert, M. G. Spencer, and M. H. Rümmeli. "A universal transfer route for graphene." In: *Nanoscale* 6.2 (2014), pp. 889–896. ISSN: 2040-3372. DOI: 10.1039/c3nr04739c.

[58] L. Liu, X. Liu, Z. Zhan, W. Guo, C. Xu, J. Deng, D. Chakarov, P. Hyldgaard, E. Schröder, A. Yurgens, and J. Sun. "A Mechanism for Highly Efficient Electrochemical Bubbling Delamination of CVD-Grown Graphene from Metal Substrates." In: *Advanced Materials Interfaces* 3.8 (2016), pp. 1–10. ISSN: 21967350. DOI: 10.1002/admi.201500492.

[59] J. Sun, X. Fan, W. Guo, L. Liu, X. Liu, J. Deng, and C. Xu. "Mechanism of electrochemical delamination of two-dimensional materials from their native substrates by bubbling." In: *Sensors (Switzerland)* 15.12 (2015), pp. 31811–31820. ISSN: 14248220. DOI: 10.3390/s151229888.

[60] G. Fisichella, S. Di Franco, F. Roccaforte, S. Ravesi, and F. Giannazzo. "Microscopic mechanisms of graphene electrolytic delamination from metal substrates." In: *Applied Physics Letters* 104.23 (2014). ISSN: 00036951. DOI: 10.1063/1.4882165.

[61] C. J. L. De La Rosa, J. Sun, N. Lindvall, M. T. Cole, Y. Nam, M. Löffler, E. Olsson, K. B. K. Teo, and A. Yurgens. "Frame assisted H2O electrolysis induced H2 bubbling transfer of large area graphene grown by chemical vapor deposition on Cu." In: *Applied Physics Letters* 102.2 (2013). ISSN: 00036951. DOI: 10.1063/1.4775583.

[62] Y. Wang, Y. Zheng, X. Xu, E. Dubuisson, Q. Bao, J. Lu, and K. P. Loh. "Electrochemical delamination of CVD-grown graphene film: Toward the recyclable use of copper catalyst." In: *ACS Nano* 5.12 (2011), pp. 9927–9933. ISSN: 19360851. DOI: 10.1021/nn203700w.

[63] S. Karamat, S. Sonusen, U. Celik, Y. Uysalli, and A. Oral. "Suitable alkaline for graphene peeling grown on metallic catalysts using chemical vapor deposition." In: *Applied Surface Science* 368 (2016), pp. 157–164. ISSN: 01694332. DOI: 10.1016/j.apsusc.2016.01.220.

[64] K. Verguts, K. Schouteden, C.-H. Wu, L. Peters, N. Vrancken, X. Wu, Z. Li, M. Erkens, C. Porret, C. Huyghebaert, C. Van Haesendonck, S. De Gendt, and S. Brems. "Controlling water intercalation is a key to a direct graphene transfer." In: *ACS applied materials and interfaces* (2017). DOI: 10.1021/acsami.7b12573.

[65] I. Childres, L. Jauregui, W. Park, H. Cao, and Y. Chen. "Raman Spectroscopy of Graphene and Related Materials." In: *Nova Science publishers* (2013), pp. 1–20. DOI: 10.1016/B978-0-444-53175-9.00016-7.

[66] A. C. Ferrari and D. M. Basko. "Raman spectroscopy as a versatile tool for studying the properties of graphene." In: *Nature Nanotechnology* 8.4 (2013), pp. 235–246. ISSN: 1748-3387. DOI: 10.1038/nnano.2013.46.

[67] Y. Liu, Z. Liu, W. S. Lew, and Q. J. Wang. "Temperature dependence of the electrical transport properties in few-layer graphene interconnects." In: *Nanoscale research letters* 8.1 (2013), p. 335. ISSN: 1931-7573. DOI: 10.1186/1556-276X-8-335.

[68] C. Neumann, S. Reichardt, P. Venezuela, M. Drögeler, L. Banszerus, M. Schmitz, K. Watanabe, T. Taniguchi, F. Mauri, B. Beschoten, S. V. Rotkin, and C. Stampfer. "Raman spectroscopy as probe of nanometre-scale strain variations in graphene." In: *Nature Communications* 6.May (2015), p. 8429. ISSN: 2041-1723. DOI: 10.1038/ncomms9429. eprint: arXiv:1406.7771v2.

[69] J. Sun, S. Deng, W. Guo, Z. Zhan, J. Deng, C. Xu, X. Fan, K. Xu, W. Guo, Y. Huang, and X. Liu. "Electrochemical bubbling transfer of graphene using a polymer support with encapsulated air gap as permeation stopping layer." In: *Journal of Nanomaterials* 2016 (2016). ISSN: 16874129. DOI: 10.1155/2016/7024246.

[70] W. Kern and J. E. Soc. "The Evolution of Silicon Wafer Cleaning Technology." In: *Journal of the Electrochemical Society* 137.6 (1990), pp. 1887–1892. ISSN: 00134651. DOI: 10.1149/1.2086825.

[71] Y. Ahn, J. Kim, S. Ganorkar, Y.-H. Kim, and S.-I. Kim. "Thermal annealing of graphene to remove polymer residues." In: *Materials Express* 6.1 (2016), pp. 69–76. ISSN: 21585849. DOI: 10.1166/mex.2016.1272.

[72] G. M. Ku, E. Lee, B. Kang, J. H. Lee, K. Cho, and W. H. Lee. "Relationship between the dipole moment of self-assembled monolayers incorporated in graphene transistors and device electrical stabilities." In: *RSC Adv.* 7.43 (2017), pp. 27100–27104. ISSN: 2046-2069. DOI: 10.1039/C7RA03865H.

[73] J. Y. Hong, Y. C. Shin, A. Zubair, Y. Mao, T. Palacios, M. S. Dresselhaus, S. H. Kim, and J. Kong. "A Rational Strategy for Graphene Transfer on Substrates with Rough Features." In: *Advanced Materials* 28.12 (2016), pp. 2382–2392. ISSN: 15214095. DOI: 10.1002/adma.201505527.

[74] W. Gao, P. Xiao, G. Henkelman, K. M. Liechti, and R. Huang. "Interfacial adhesion between graphene and silicon dioxide by density functional theory with van der Waals corrections." In: *Journal of Physics D: Applied Physics* 47.25 (2014), p. 255301. ISSN: 0022-3727. DOI: 10.1088/0022-3727/47/25/255301.

[75] A. N. Rudenko, F. J. Keil, M. I. Katsnelson, and A. I. Lichtenstein. "Interfacial interactions between local defects in amorphous SiO_2 and supported graphene." In: *Physical Review B - Condensed Matter and Materials Physics* 84.8 (2011), pp. 1–9. ISSN: 10980121. DOI: 10.1103/PhysRevB.84.085438.

[76] S. Shin, S. Kim, T. Kim, H. Du, K. S. Kim, S. Cho, and S. Seo. "Graphene transfer with self-doping by amorphous thermoplastic resins." In: *Carbon* 111 (2017), pp. 215–220. ISSN: 00086223. DOI: 10.1016/j.carbon.2016.09.077.

[77] T. Li and Z. Zhang. "Substrate-regulated morphology of graphene." In: *Journal of Physics D: Applied Physics* 43.7 (2010), p. 075303. ISSN: 0022-3727. DOI: 10.1088/0022-3727/43/7/075303.

[78] M. Kim, A. Shah, C. Li, P. Mustonen, J. Susoma, F. Manoocheri, J. Riikonen, and H. Lipsanen. "Direct transfer of wafer-scale graphene films." In: *2D Materials* 4.3 (2017), p. 035004. ISSN: 2053-1583. DOI: 10.1088/2053-1583/aa780d.

[79] C.-C. Yang and W.-C. Chen. "The structures and properties of hydrogen silsesquioxane (HSQ) films produced by thermal curing." In: *Journal of Materials Chemistry* 12.4 (2002), pp. 1138–1141. ISSN: 09599428. DOI: 10.1039/b107697n.

[80] M. J. Loboda and G. a. Toskey. "Understanding hydrogen silsesquioxane-based dielectric film processing." In: *Solid State Technology* 41.5 (1998), pp. 99–101. ISSN: 0038-111X.

[81] J. Kim, W. Chao, B. Griedel, X. Liang, M. Lewis, D. Hilken, and D. Olynick. "Understanding the base development mechanism of hydrogen silsesquioxane." In: *Journal of Vacuum Science & Technology B: Microelectronics and Nanometer Structures* 27.6 (2009), p. 2628. ISSN: 10711023. DOI: 10.1116/1.3250261.

[82] P. Blake, E. W. Hill, A. H. Castro Neto, K. S. Novoselov, D. Jiang, R. Yang, T. J. Booth, and A. K. Geim. "Making graphene visible." In: *Applied Physics Letters* 91.6 (2007), pp. 2007–2009. ISSN: 00036951. DOI: 10.1063/1.2768624. eprint: 0705.0259.

[83] J. Song, F.-Y. Kam, R.-Q. Png, W.-L. Seah, J.-M. Zhuo, G.-K. Lim, P. K. H. Ho, and L.-L. Chua. "A general method for transferring graphene onto soft surfaces." In: *Nature nanotechnology* 8.5 (2013), pp. 356–362. ISSN: 1748-3395. DOI: 10.1038/nnano.2013.63.

[84] Y. Zhu, S. Murali, W. Cai, X. Li, J. W. Suk, J. R. Potts, and R. S. Ruoff. "Graphene and graphene oxide: Synthesis, properties, and applications." In: *Advanced Materials* 22.35 (2010), pp. 3906–3924. ISSN: 09359648. DOI: 10.1002/adma.201001068.

[85] M. Hayyan, F. S. Mjalli, M. A. Hashim, I. M. AlNashef, and T. X. Mei. "Investigating the electrochemical windows of ionic liquids." In: *Journal of Industrial and Engineering Chemistry* 19.1 (2013), pp. 106–112. ISSN: 1226086X. DOI: 10.1016/j.jiec.2012.07.011.

[86] S. Lower. *24.4: The Nernst Equation*. 2017. URL: https://chem.libretexts.org/Textbook{_}Maps/General{_}Chemistry{_}Textbook{_}Maps/Map{\%}3A{_}Chem1{_}(Lower)/16{\%}3A{_}Electrochemistry/24.04{\%}3A{_}The{_}Nernst{_}Equation (visited on 07/18/2017).

Appendix A

Target Substrate

Since one of the goals of this thesis is to implement graphene in CMOS technology, the target substrates used were always silicon/silicon dioxide (Si/SiO_2). Here it is mandatory a certain thickness for SiO_2 so graphene can make contrast with the substrate making it possible to be seen in the optical microscope and even noticed by naked eye (see fig. A.1). The contrast is optimal when SiO_2 has a thickness of 90 or 300 nm due to increased optical path and due to the opacity of graphene [82].

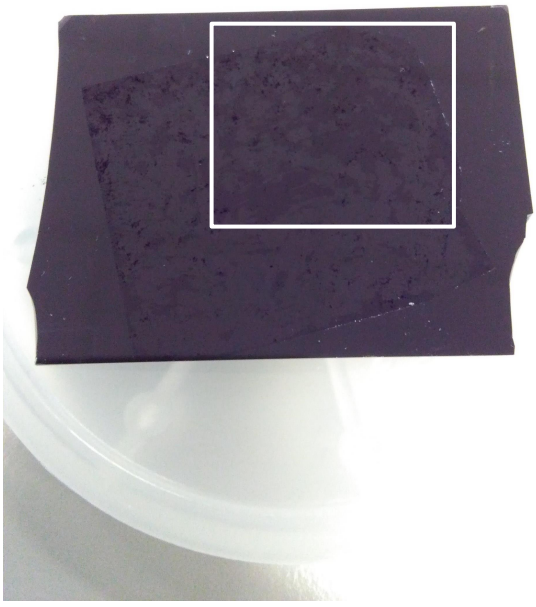

Figure A.1: Graphene visible on a Si/SiO_2 substrate. A white square marks where there is the most part of graphene, visible by the darker parts.

Moreover, two treatments were applied to the Si/SiO_2 substrate so it could gain an ideal characteristic for the up following transfers.

- For the standard wet- and dry- transfer the substrate should be hydrophilic. This feature not only allows an easier fishing in the wet-transfer but also avoids solvent intercalation between the substrate and the graphene in both transfers. The treatment to achieve this condition is by immersing the substrate in a solution H_2O:

NH_4: H_2O_2 (3:1:1 for volume ratio) for 10 minutes gaining a water contact angle of < 10 °.

- For the direct transfer the substrate should be hydrophobic. In this case it is important so it can avoid water intercalation at the same time that graphene is being transferred. The substrate is treated with a perfluorodecyltrichlorosilane (FDTS) layer making a water contact angle of 109.5 °.

Appendix B

Support Material

The support layer is rather a very important film that protects the graphene during a typical transfer. Polymers are frequently used due their flexible and rigid features and can be spin coated on top of the Pt foils, aiding and making the dry-and wet-transfers possible. The polymeric films used in this work were PMMA, PDMS and PC, which have their structures depicted in Figure B.1.

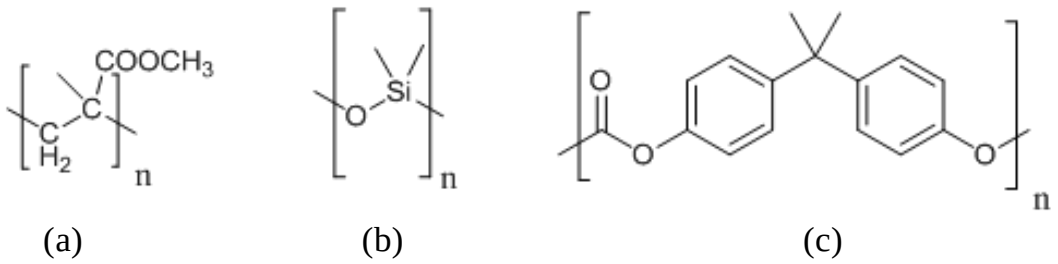

Figure B.1: Skeletal formula of (a) PMMA, (b) PDMS and (c) PC.

In the case of PC, it was used a solution of 2% dissolved in chloroform. The strong adhesion between graphite and PC has already been reported [83] and it was spin coated on top of graphene at 1500 rotations per minute (rpm) for 60 seconds. Then it was baked at 50 °C for 5 minutes to evaporate the solvents. After the reported transfers, PC can easily be removed by dichloromethane (DCM) at 35 °C for 2 hours, leaving an uniform and flat surface with few residues.

With PMMA, it was used a solution of 4% dissolved in anisole. It can easily be spin coated on top of graphene and has a good adhesion with it [84]. Here, the conditions were 1000 rpm for 60 seconds. Then a bake of 135 °C for 10 minutes is done to completely remove the solvents. After the transfer, PMMA can be removed either by acetone or by annealing. The last option gives better results because avoids solvent intercalation and provides a stable and controlled method to clean graphene. In the procedure, the heating rate is done at 1 °C min^{-1}, maintain at 400 °C for 4 hours and then cooled down to room temperature at a rate of 1 degree C min^{-1}. However, there is still a lot of polymer contamination after the annealing.

PDMS is used as an extra supporting layer that assists specifically the dry-transfer due its larger thickness and a lesser brittle nature comparing with the remaining polymers.

This way graphene can endure the required handling for a dry-transfer without heavy damage. The fact that it is a viscoelastic material means it can be slowly peeled off when increasing the temperature to around 130 °C. However, when using PDMS to bond and de-bond graphene with the target substrate graphene is usually torn due the incomplete adhesion between graphene and the substrate [73].

HSQ is not a support layer and it is used as target substrate but will be detailed here since it is also a polymer. It is spin-coated on the target substrate at 2500 rpm for 31 seconds and then baked at 150 °C for 2 minutes. After this it is still in its cage form (Figure B.2a) and only after curing partially transforms into the network form (Figure B.2b), the SiO_2. The curing temperature would be 400 °C to achieve a higher conversion rate [79].

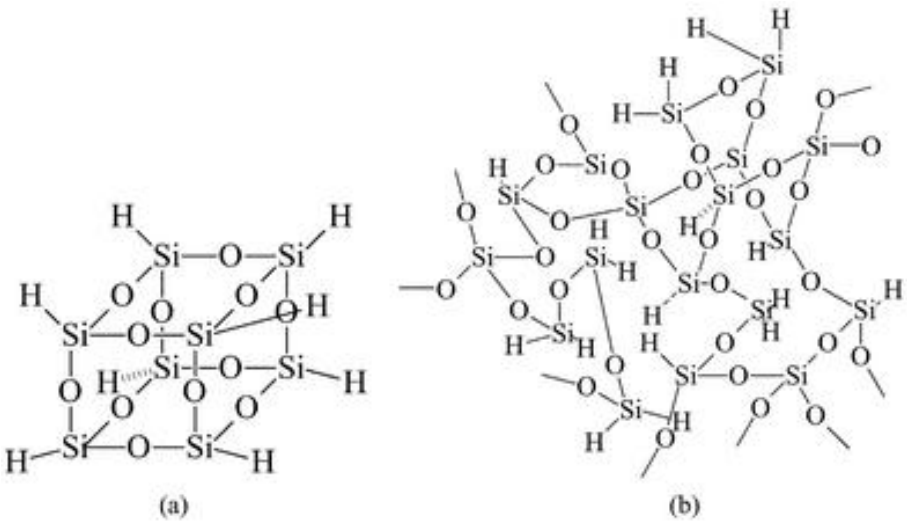

Figure B.2: Chemical structures of HSQ: (a) cage form, (b) network form. From [79].

Appendix C

Calculations for the reduction/oxidation potential

An EW is one of the most important characteristics to be identified for solvents and electrolytes used in electrochemical applications. Essentially, is the potential range between which the tested substance does not get oxidized nor reduced, i.e., it is inert within this range [85]. In this case study, an EW for water is needed with the potentials for reducing and oxidizing the water. To calculate those potentials, it is used the Pourbaix diagram that correlates the potential needed with the pH of the solution. According to the diagram there is two slopes responsible for the redox reaction: $E = 1.229 - 0.059pH$ for oxidation and $E = -0.059pH$ for reduction [86]. Using the pH values represented in table 3.1, the redox potentials are easily calculated (see Table C.1) and an EW for each electrolyte can be made. However, for a simpler and easier interpretation, only three water EW were made which includes acidic, neutral and alkaline conditions. Figure C.1 depicts those EW with an approximation of the potential values.

Table C.1: Reduction/oxidation potentials of water depending on the pH of the solution.

Electrolyte	**Reduction potential (V)** $E_{red} = -0.059 * pH$	**Oxidation potential (V)** $E_{oxi} = 1.229 - 0.059 * pH$
NaOH	-0.79	0.44
TMAH	-0.77	0.46
TEAH	-0.77	0.46
NH_4OH	-0.67	0.56
$NaNO_3$	-0.41	0.81
Na_2SO_4	-0.41	0.81
Na_2SO_3	-0.41	0.81
K_2SO_4	-0.41	0.81
TMACl	-0.41	0.81
NaCl	-0.41	0.81
HNO_3	-0.041	1.27
H_2SO_4	-0.024	1.21
$Ce(SO_4)_2$	-0.024	1.21

Afterwards, the next step is to calculate the reduction/oxidation potential for each cation/anion involved in the experiment by the Nernst equation (eq. C.1) and, as this thesis defends, check if it is in or outside the EW.

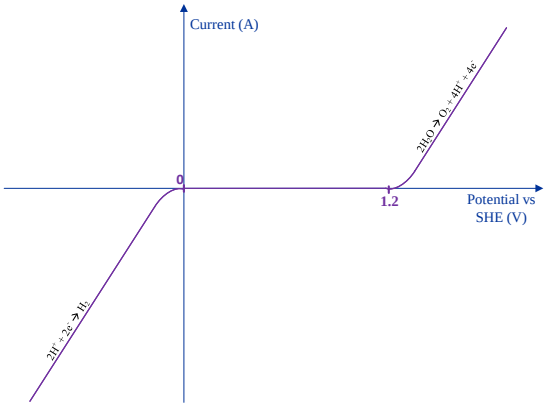

(a)

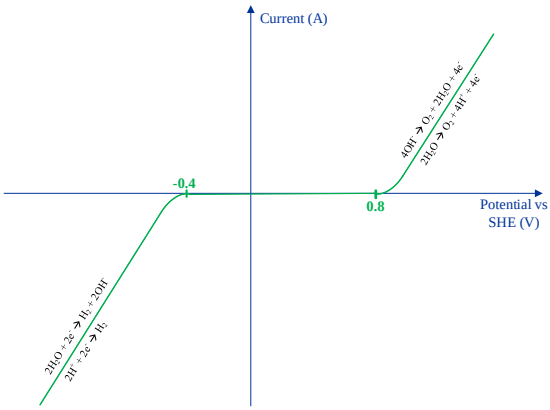

(b)

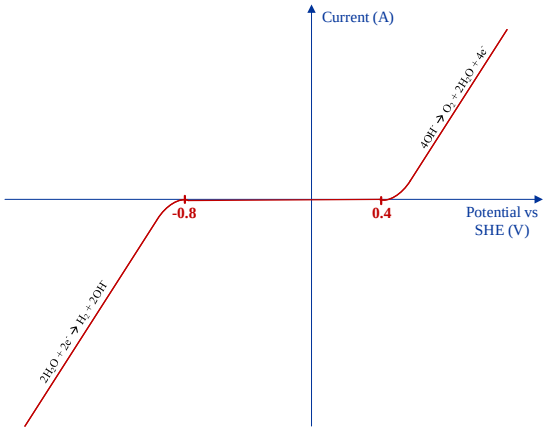

(c)

Figure C.1: Electrochemical window of water for: (a) acidic solutions, (b) neutral solutions and (c) alkaline solutions.

$$E_{red/ox} = E^0_{red/oxi} - \frac{0.059}{n} \log_{10} Q \tag{C.1}$$

Where $E_{red/ox}$ is the reduction/oxidation potential, $E^0_{red/ox}$ is the standard reduction/oxidation potential, n is the number of electrons transferred in the half-reaction and Q is the reaction quotient, all at 25 °C. Table C.2 demonstrates all data needed for the calculation of $E_{red/ox}$.

Table C.2: Reduction/oxidation potentials of the remaining ions.

Half-reaction	**Standard Potential (V)**	**n**	**Q**	**$E_{red/oxi}$ (V)**
$K^+ + e^- \longrightarrow K$	-2.93	1	5	-2.97
$Na^+ + e^- \longrightarrow Na$	-2.71	1	5	-2.75
$SO_3{}^{2-} + 2OH^- \longrightarrow SO_4{}^{2-} + H_2O + 2e^-$	-0.94	2	1	-0.94
$2Cl^- \longrightarrow Cl_2 + 2e^-$	1.40	2	25	1.36
$Ce^{4+} + e^- \longrightarrow Ce^{3+}$	1.44	1	1	1.44
$SO_4{}^{2-} \longrightarrow S_2O_8{}^{2-} + 2e^-$	1.96	2	1	1.96